Upwelling and the persistence of coral-reef frameworks in the eastern tropical Pacific

Ian C. Enochs[a,*], Lauren T. Toth[b], Amanda Kirkland[c], Derek P. Manzello[a], Graham Kolodziej[a,d], John T. Morris[a,d], Daniel M. Holstein[e], Austin Schlenz[a,d], Carly J. Randall[f], Juan L. Maté[g], James J. Leichter[h], Richard B. Aronson[i]

[a] NOAA, Atlantic Oceanographic and Meteorological Laboratory, Ocean Chemistry and Ecosystem Division, 4301 Rickenbacker Causeway, Miami, FL 33149, USA

[b] U.S. Geological Survey, St. Petersburg Coastal and Marine Science Center, 600 4th Street, St. Petersburg, FL 33701, USA

[c] The University of New Orleans, 2000 Lakeshore Drive, New Orleans, LA 70148, USA

[d] University of Miami, Cooperative Institute for Marine and Atmospheric Studies, 4600 Rickenbacker Causeway, Miami, FL 33149, USA

[e] Louisiana State University, Department of Oceanography and Coastal Sciences, College of the Coast and Environment, 2259 Energy, Coast and Environment Building, Baton Rouge, LA 70803, USA

[f] Australian Institute of Marine Science, PMB No. 3, Townsville, Queensland 4810, Australia

[g] Smithsonian Tropical Research Institute, Apartado Postal 0843-03092, Panamá, República de Panamá

[h] Scripps Institution of Oceanography, University of California San Diego, 8635 Kennel Way, La Jolla, California 92037, USA

[i] Florida Institute of Technology, 150 West University Boulevard, Melbourne, Florida 32901, USA

[*]**Corresponding author:** Ian C. Enochs, ian.enochs@noaa.gov

for publication in
Ecological Monographs

Abstract

In an era of global change, the fate and form of reef habitats will depend on shifting assemblages of organisms and their responses to multiple stressors. Multiphyletic assemblages of calcifying and bioeroding species contribute to a dynamic balance between constructive and erosive processes, and reef-framework growth occurs only when calcium-carbonate deposition exceeds erosion. Each contributing species exhibits a unique combination of environmental sensitivities, trophic needs, and competitive abilities, making the net outcome of their habitat-altering behavior difficult to predict. In this study, standardized blocks of clean, massive *Porites* were placed at six reef sites in the eastern tropical Pacific, in the strongly and more-weakly upwelling Gulfs of Panamá (GoP) and Chiriquí (GoC), respectively. Sites were instrumented to characterize the unique thermal and carbonate-chemistry conditions of each gulf. Satellite products were used to examine differences in sea-surface productivity, and surveys were conducted to quantify the abundance of important grazing taxa. After two years *in situ*, the *Porites* blocks were collected and scanned using high-resolution computed tomography to volumetrically quantify both endolithic and epilithic habitat alteration. Scan-volumes were further classified into functional groups according to morphology to quantify external bioerosion by fish and sea urchins, as well as the calcifying and bioeroding activity of crustose coralline algae, scleractinian corals, mollusks, annelids, and barnacles. The GoP, which has higher productivity, cooler temperatures, and periodically lower pH conditions, had higher rates of macroboring, but also higher rates of calcification. These unexpectedly higher rates of calcification in the GoP were a result of high recruitment of suspension-feeding taxa, particularly barnacles and vermiform fauna that have poor reef-forming potential. External bioerosion by grazers was the dominant process influencing these dead coral substrates across both gulfs,

contributing to higher rates of net erosion in the GoC and underscoring the important roles that urchins and fish play in not just removing algae on reefs, but also eroding reef habitat. Ultimately these findings reveal that the trophic requirements of habitat-altering taxa are closely tied to reef-framework stability, and that environmental conditions conducive to carbonate precipitation are not necessarily those that will lead to habitat persistence.

Key words: bioerosion, calcification, coral reef, eutrophication, habitat loss, upwelling

Introduction

The high biodiversity and biomass for which coral reefs are well known are inexorably linked to a complex three-dimensional structure that provides essential shelter and habitat for the associated biota. This reef framework is primarily composed of the calcium carbonate skeletons of scleractinian corals, but other plants and animals, including crustose coralline algae (CCA), mollusks, and hydrocorals form, bind, and cement these structures into place (Perry and Hepburn 2008). Biological breakdown of reef carbonates, termed bioerosion, occurs at many different scales (Glynn and Manzello 2015). Diverse microboring species dissolve networks of microscopic cavities (<100 μm), whereas macroboring fauna use mechanical and chemical techniques to create boreholes and anastomosing chambers that can be 1 cm in diameter. On the surface of the reef, epilithic bioerosion occurs as animals such as parrotfish and sea urchins scrape and bite away at carbonates while grazing for food.

Quantifying the balance of these accretionary and erosive processes, such as through the use of bioerosion accretion replicates (BARs; Enochs et al. 2016), is paramount to predicting the persistence of reef habitats (Glynn and Manzello 2015) and ultimately the goods and services supplied by these important ecosystems (Moberg and Folke 1999). Large declines in coral cover

over the last several decades (Gardner et al. 2003, De'ath et al. 2012) have been accompanied by a loss of reef-framework (Alvarez-Filip et al. 2009), as rates of erosion have begun to exceed calcification. Today, many reefs exhibit diminished growth potential and, going forward, may not be able to keep up with rising sea levels (Yates et al. 2017, Perry et al. 2018).

Factors contributing to this dire situation are numerous and range in scale from acute regional stressors to chronic global problems. With respect to accretion, extreme temperature has led to the mortality of important calcifying taxa (Baker et al. 2008, Lirman et al. 2011), while ocean acidification (OA) is slowing the rate at which many species can deposit calcium carbonate (Chan and Connolly 2013). High primary productivity and reduced macroalgal grazing can also lead to competitive exclusion, reduced settlement, and depressed calcification of corals, which generally thrive in oligotrophic waters (Tomascik and Sander 1985, McCook 1999).

Bioerosion is similarly dynamic, and the factors that impede coral calcification often accelerate erosion as well. For example, mass coral die-offs related to thermal anomalies have been correlated with higher abundances of bioeroding sponges due to the increased availability of suitable dead coral skeletons for settlement (Chaves-Fonnegra et al. 2018), and OA is known to accelerate the rate at which bioeroders chemically dissolve reef substrates (Tribollet et al. 2009, Enochs et al. 2016). The prevalence of heterotrophic macroboring species has been shown to be elevated in eutrophic waters with elevated bacterioplankton food sources (Rose and Risk 1985), whereas autotrophic microboring taxa may respond directly to elevated inorganic nutrients (Carreiro-Silva et al. 2009).

The magnitude and direction of the responses of both reef accretion and bioerosion to environmental changes are, however, complicated by real-world complexity. Different species and functional groups may respond differently to stress based on environmental tolerances,

behaviors, or trophic requirements (Enochs and Glynn 2016). For example, whereas OA may accelerate microboring (Tribollet et al. 2009), it is not presently thought to directly alter external bioerosion by fish and urchins, demonstrating the complexity of how different groups of bioeroders may respond to environmental stressors. Furthermore, species and functional groups do not exist in isolation; they can compete for space or food, or even prey upon each other. Addressing the impact of a single stressor on multiple interacting taxa may, therefore, lead to a myopic view of taxon-level responses. Species considered a priori to be environmentally resilient may be strongly and unexpectedly impacted, and the strong, stressor-specific responses of an individual taxon may not manifest in detectable alteration to the ecosystem. These inherent non-linear feedbacks and quirks of complexity may ultimately drive ecosystem outcomes that are different from the simple sum of the parts. For example, with respect to OA-driven acceleration of microboring, when the impact of external bioerosion was considered simultaneously, the effect of OA was no longer detectable, potentially due to grazers removing the upper millimeter of substrate, where much of the phototrophic microboring occurred (Enochs et al. 2016). Similarly, environmental stressors rarely occur in isolation. Simultaneous exposure to multiple stressors can lead to non-additive responses, including both synergistic and antagonistic reactions that are difficult to predict (Darling and Côté 2008).

To better understand the fate of reef habitats in response to environmental change, it is important to consider co-occurring stressors influencing multiple, interacting species. Naturally extreme environments can provide insights into how ecosystems will respond to anthropogenic stress, while incorporating levels of complexity that are orders of magnitude higher than currently can be replicated in a laboratory setting. For example, natural CO_2 enrichment due to volcanic vents can force coral reefs into alternative states or produce remarkable diversity,

depending on a combination of local factors (Fabricius et al. 2011, Inoue et al. 2013, Enochs et al. 2015). Careful characterization of communities within these environments can help to reveal the processes underlying resilience and help to predict persistence, alteration, or collapse (Enochs et al. 2016).

Previous studies have used carbonate blocks and two-dimensional image analysis to investigate how multispecies assemblages influence reef-habitat persistence (Davies and Hutchings 1983, Peyrot-Clausade et al. 1992, Chazottes et al. 1995, Reaka-Kudla et al. 1996, Tribollet et al. 2002, Tribollet and Golubic 2005). More recently, micro-computed tomography (CT) has been applied to carbonate blocks to measure changes in net accretion and erosion volumetrically (Silbiger et al. 2014), as well as the individual contribution of functional groups (Enochs et al. 2016). Here we examine these processes within a natural upwelling gradient across two Panamanian gulfs in the eastern tropical Pacific (ETP), which differ in temperature, productivity, and carbonate-chemistry dynamics (Glynn and Maté 1997, Manzello et al. 2008, Randall et al. 2020). We deployed blocks of dead coral skeletons for two years and used CT scanning and three-dimensional volumetric delineation to characterize the impacts of a multiphyletic assemblage of organisms on a natural reef substrate within each of these gulfs. We used these data to evaluate the likelihood of reef-habitat persistence under global change in oceanographically dynamic environments like the ETP. This study, to our knowledge, represents the first analysis in which CT was used to three-dimensionally quantify not only functional groups, but also the high-level taxonomic composition of organisms contributing to macroboring and accretion.

Methods

Three coral reef sites were chosen in each of the two gulfs along the Pacific coast of Panamá: Saboga, Contadora, and Pedro González in the Gulf of Panamá (GoP), which experience strong seasonal upwelling; and Uva, Canales de Tierra, and Coiba in the Gulf of Chiriquí (GoC), which experiences weak upwelling events and has historically been considered a non-upwelling system (Fig. 1). Upwelling in the GoP occurs during the dry season from mid-December through April and is associated with strong trade winds moving across the Isthmus of Panamá (Glynn and Maté 1997, D'Croz and O'Dea 2007).

Environmental and ecological data

Temperature loggers (HOBO Pro v2, Onset, Cape Cod, Massachusetts, USA) were deployed at each site and recorded seawater temperature every 15 minutes from March 2016 to March 2018. Records were used to calculate daily means at the site level and were averaged to obtain daily means for each gulf. Monthly mean chlorophyll *a* was derived from satellite products (MODIS, 4.6 km; Hu et al. 2012) for each site, and for the entirety of each gulf, in order to describe seasonal variation in productivity over this same period. Satellite data were not obtained during months in which the sea surface was not visible due to cloud cover. Long-term pCO_2 loggers (SAMI-CO2; Sunburst Sensors, Missoula, Montana, USA) were deployed at one site per gulf (Saboga and Uva in the GoP and GoC, respectively) in order to describe carbonate-chemistry dynamics. The periods of successful data collection for the carbonate chemistry (GoP, August 2015–June 2016 and March–September 2018; GoC, August 2015–April 2016 and March–October 2018) did not coincide completely with the other measured parameters but captured the full seasonal cycle in CO_2 associated with the upwelling gradient. Parrotfish and sea-urchin surveys (n = 4–8) were conducted within 4 x 25 m belt transects haphazardly placed

(at least 5 m apart) within the same depth zone as the BARs at each site in the Spring of 2018 and 2019. A trained observer first swam slowly along each transect and recorded the number and species of parrotfishes observed within the 4 x 25 m area. A second observer then recorded the number and species of urchins within the same area, being careful to look within cryptic areas of the reef framework. Because we did not estimate the sizes of these taxa, the data do not provide a direct measurement of grazing intensity. Instead, we utilized these data as an estimate of differences in grazer densities between gulfs.

Bioerosion accretion replicates

Bioerosion accretion replicates were constructed from cleaned and dried *Porites* skeletons to examine the persistence of reef carbonates. Standardized slices of *Porites* skeletons were made by vertically bisecting cylinders (10 cm diameter x 1.5 cm thick) that were cut from cores in the U.S. Geological Survey Core Archive that originated from Hawaii (access information online).[11] The semicircular coral slices were epoxied to larger PVC discs, with a hole for attachment drilled in each PVC disc (Fig. 2A). Assembled BARs were dried at 60 °C for 24 h, weighed on an analytical balance (0.0001 g precision; Ohaus, Parsippany, New Jersey, USA) and scanned using CT (Volume Zoom, Siemens, Munich, Germany, 0.1-mm slice thickness).

Bioerosion accretion replicates were affixed to existing reef framework, dominated by branching corals in the genus *Pocillopora*, using rebar stakes and hose clamps (Fig. 2A). At each site, 10 BARs were haphazardly positioned within the upper reef slope (˜3 m below mean sea level), separated by ˜5 m, over a total planar area less than 1,000 m^2. BARs were collected after incubating for two years in the field, from March 2016 to March 2018. Photos were taken of the top of each BAR in March 2018 and the epibenthic cover was classified under 30 random points

using CoralNet (Beijbom et al. 2015). The epibenthic categories were annelids, barnacles, mollusks, macroalgae, turf algae, CCA, bare space, and other. Organic material was removed using dilute (15%) hydrogen peroxide for 48 h and gentle abrasion, to avoid dislodging fragile calcified structures. The PVC bases were more rigorously scrubbed to remove all calcifying material that had not originally settled directly on the carbonate block. The blocks were then dried at 60 °C for 24 h and reweighed on an analytical balance.

Bioerosion accretion replicates were CT-scanned following deployment, and the bioerosion and/or accretion by functional groups was digitally isolated using Amira software (Thermo Fisher Scientific, Waltham, Massachusetts, USA; see Enochs et al. 2016). Briefly, new carbonate materials on the surface of the BARs were classified as accretion, whereas voids formed within the BAR were attributed to macroboring. External bioerosion was determined as the change in the external volume of the BAR, not inclusive of newly accreted substrate. It is not possible to determine if this volume contained macroboring or new accretion prior to removal by grazers, and the contributions of these functional groups may therefore be underrepresented. The density of the remaining *Porites* skeleton, which was not discernibly eroded by macroborers, was interpolated from mean intensity (in Houndsfield units), calibrated against the intensity of six aragonite-density standards that were scanned using the same scan settings (Enochs et al. 2016). Changes in sample density after deployment reflect the net outcome of processes influencing carbonate skeletons, such as cementation, as well as biotic and abiotic dissolution, on a finer scale than detected using volumetric quantification of CT scans.

Accretion and macroboring were further classified according to the taxonomy of the causative agents as inferred from their taphonomic signatures. Accretion was split into material added by CCA, barnacles, vermiform fauna (inclusive of polychaetes and vermetid gastropods),

and corals. Macroboring was divided into bivalve excavations and worm-like burrows. The latter burrows were simply labeled “annelid” as we were unable to assess the taxonomy of those traces. Given the two-year BAR deployment, however, we assume that the majority of this erosion was due to the activity of polychaetes, which are more often present in the earlier stages of macroborer succession than sipunculid worms (reviewed in Hutchings 2008). Observations from the Galápagos support this assumption (Reaka-Kudla et al. 1996).

Statistical analysis

All statistical analyses were run using R (RCore Team 2008) with RStudio (RStudio Team 2015). Differences in total grazer density (urchins and parrotfish) were tested between gulfs using Kruskal-Wallis rank-sum tests. Generalized linear models were run on the response variables (both carbonate alteration and surface cover) using the most appropriate distribution, determined using the fitdistrplus package (Delignette-Muller and Dutang 2015). For the purposes of analysis, data were adjusted when necessary to positive proportions (for gamma distributions). Plots were created using the ggplot2 package (Wickham 2016). The lubridate package (Grolemund and Wickham 2011) was employed to visualize time-series data. Summary statistics for environmental conditions for the sites and gulfs were calculated using plyr (Wickham 2011).

Principal component analyses (PCAs) were used to explore trends in sites and, separately, BARs in multivariate space with the vegan package (Oksanen et al. 2019). Environmental variables, including mean temperature, variance in temperature, chlorophyll *a* concentration, and the densities of grazing taxa were used to construct ordination axes, and sites were scored. In a separate PCA, accretion/erosion rates of different functional groups were used to construct ordination axes, and each BAR was scored.

Results

Site and gulf characteristics

Dry-season upwelling in the GoP was accompanied by a drop in temperature to a low of 17.9 °C and an average of 25.1° ± 2.5 °C (mean ± SD), compared with a wet-season average of 28.6° ± 0.6 °C (Fig. 3; Appendix S1: Table S1). Temperatures in the GoC remained relatively stable and were similar to those observed during the wet season in the GoP, with averages of 28.9° ± 0.7°C and 28.8° ± 0.7°C in the dry and wet seasons, respectively (Fig. 3; Appendix S1: Table S1). Productivity, from satellite-derived chlorophyll *a*, was higher in the GoP throughout the year and peaked in the dry season, concurrent with low water temperatures (Fig. 3; Appendix S1: Table S1). CO_2 dynamics were more complex and highly variable, although they generally mirrored gulf-averaged productivity in the GoP (Fig. 3; Appendix S1: Table S1). Interestingly, short-term variability in pCO_2 (over hours to days) was qualitatively greater in the GoC (Fig. 3), although this was not captured in the reported variances due to the greater seasonal fluctuations (Appendix S1: Table S1). Sea-urchin assemblages were dominated by *Diadema mexicanum*, which exhibited especially high densities at Contadora (Appendix S1: Fig. S1, Table S1). The most abundant parrotfish species was *Scarus ghobban*, which reached its highest (but also highly variable) densities at Coiba (0.17 ± 0.21 individuals m^{-2}; Appendix S1: Fig. S1, Table S1). Although there was some spatial variability in the densities of some of the scarcer grazing taxa, no significant differences were detected between gulfs in total sea urchin densities ($\chi^2 = 1.6169$, df = 1, $P = 0.2035$) or total parrotfish densities ($\chi^2 = 0.95791$, df = 1, $P = 0.3277$; Appendix S1: Fig. S1, Table S1).

Epibenthic cover

Algae comprised the majority of the epibenthic cover of the BARs. There were no significant differences in algal cover between the gulfs, with only Uva and Coiba falling out as having significantly higher cover within the GoC (Appendix S1: Fig. S2, Tables S2, S3). The cover of CCA and bare substrate were also not significantly different between gulfs and no among-site differences were detected (Appendix S1: Fig. S2, Tables S2, S3). Sessile invertebrate suspension-feeders, including barnacles, annelids, and mollusks, were present primarily in the GoP where productivity was higher, although their distribution was highly variable. As a result, there were no significant differences in their abundances among sites or gulfs (Appendix S1: Fig. S2, Tables S2, S3).

Carbonate alteration

Bioerosion accretion replicates in the GoC lost significantly more carbonate material by mass (-1,328.2 ± 1,974.0 g m^{-2} yr^{-1}; mean ± SD) than in the GoP (-232.4 ± 861.1 g m^{-2} yr^{-1}; P = 0.0005), and there were no significant among-site differences detected within gulfs (Fig. 4; Appendix S1: Tables S4, S5). The density of the dead and unbored *Porites* skeleton, however, exhibited the opposite pattern, with a significantly higher density increase in the GoC (103.9 ± 54.2 g m^{-2} yr^{-1}) than in the GoP (31.8 ± 54.6 g m^{-2} yr^{-1}; P = 0.0003; Fig. 4; Appendix S1: Tables S4, S5). Again, there were no significant differences detected among sites (Fig. 4; Appendix S1: Tables S4, S5). There was a strong relationship between net change in mass and volume within each gulf (Fig. 4), and the total net erosion by volume was similarly greater in the GoC (-1,457.8 ± 1,030.7 cm^3 m^{-2} yr^{-1}) than the GoP (-794.3 ± 669.1 cm^3 m^{-2} yr^{-1}; Fig. 5; Appendix S1: Tables S4, S5).

Contributing to these trends in net mass and volume change, accretion was significantly lower in the GoC than in the GoP (62.8 ± 59.8 vs. 266.5 ± 166.5 cm^3 m^{-2} yr^{-1}; P = 0.0020; Fig. 5; Appendix S1: Tables S4, S5). Although the mean accretion of (autotrophic) CCA was higher in the GoP than the GoC (94.7 ± 60.6 vs. 60.2 ± 58.8 cm^3 m^{-2} yr^{-1}), this difference was not significant (P = 0.1985; Appendix S1: Fig. S3, Tables S4, S5). With respect to heterotrophs, the accretion of suspension-feeding barnacles was significantly higher in the GoP (108.8 ± 138.8 cm^3 m^{-2} yr^{-1}) than in the GoC, where they were never observed on the BARs (Appendix S1: Fig. S3, Table S4, S5). The mean accretion of vermiform fauna was similarly higher in the GoP (32.7 ± 43.5 vs. 2.5 ± 8.8 cm^3 m^{-2} yr^{-1} in the GoC), although their distribution was patchy and, as a result, the difference between gulfs was not significant (Appendix S1: Fig. S3, Tables S4, S5). Coral calcification on the BARs was not high enough to contribute strongly or significantly to carbonate production; therefore, comparisons between gulfs or among sites were not possible with these data.

Despite no significant differences detected in the densities of prominent grazing taxa observed in the *in situ* surveys, grazers removed significantly more carbonate from the surface of the BARs in the GoC (-1,473.3 ± 1,003.5 cm^3 m^{-2} yr^{-1}) than in the GoP (-871.0 ± 586.0 cm^3 m^{-2} yr^{-1}; P = 0.0062; Fig. 5; Appendix S1: Tables S4, S5). External bioerosion, measured volumetrically, was 31.1 and 4.6 times higher than macroboring in the GoC and GoP, respectively (Fig. 5; Appendix S1: Table S4). Macroboring rates were significantly higher in the GoP (-189.8 ± 118.7 vs. -47.3 ± 40.4 cm^3 m^{-2} yr^{-1} in the GoC; P = 0.0070; Fig. 5; Appendix S1: Tables S4, S5). This difference was driven by the lithophagine bivalves, which were the greatest contributors to macroboring and were significantly more destructive in the GoP (-154.7 ± 120.4 vs. -4.3 ± 10.5 cm^3 m^{-2} yr^{-1} in the GoC; Appendix S1: Fig. S4; Tables S4, S5). Annelids, by

contrast, were not significantly more prevalent in one gulf or the other (Appendix S1: Fig. S4, Tables S4, S5).

Multivariate community responses

Using environmental and grazer-abundance data, gulfs can be differentiated in PCA-space along the first PC axis, which explains 62.14% of the variance and is primarily influenced by mean temperature, variation in temperature, and chlorophyll *a* concentration at each site (Fig. 6A). Within gulfs, sites can be further distinguished along PC2, which explains 22.20% of the variance and is correlated with the density of grazing herbivores. BARs deployed at these sites differentiate in PCA-space according to gulf on the first PC axis (explaining 35.76% of the variance, Fig. 6B). Vectors largely correspond to the significant differences in functional-group responses detected between gulfs (Appendix S1: Table S5). Barnacles, CCA, and bivalve macroboring were correlated with GoP reef sites. Vermiform-fauna accretion, which appears to have differed between gulfs (Appendix S1: Fig. S3) but was not detected as significant (Appendix S1: Table S5), strongly correlates with the GoP as well (Fig. 6). Increased carbonate density correlates with the GoC. BARs further differentiate on both PC1 and PC2 to a certain degree by site, PC2 explained 17.33% of the variance and correlated with annelid erosion, which was highest on Uva reef (Fig. 6). Interestingly, external bioerosion and CCA accretion are negatively correlated and plot roughly perpendicular to gulf-differentiation in PCA space (Fig. 6).

Discussion

Detailed analysis of interacting functional groups is key to identifying the major environmental drivers influencing carbonate persistence and, ultimately, to predicting the fate of

reef habitat. We found that high external bioerosion in the ETP drives carbonate erosion, but high productivity due to upwelling favors heterotrophic benthic assemblages, accelerating macroboring and supporting less structurally stable, faster-growing calcifying animals. As BARs represent dead carbonate frameworks, our results suggest that extensive coral mortality caused by extreme or frequent perturbations, such as mass bleaching events, may ultimately be more difficult to recover from in areas of high productivity. Although gross-calcification rates may remain high, carbonate precipitation by exclusively heterotrophic species will favor the production of sediments rather than solid, habitat-forming reef frameworks.

Calcification

Historically, the calcification rates of reef-building corals have been higher in the GoC due to more favorable, less variable environmental conditions (Glynn and Macintyre 1977). Over millennial timescales, this difference has led to greater reef development in the GoC compared with the GoP (Glynn and Macintyre 1977). Reef frameworks in the GoP are largely restricted to the northern and eastern sides of islands, which experience less-extreme upwelling conditions than southern- and western-facing shorelines (Glynn and Stewart 1973). Recent evidence suggests, however, that the growth rates and coverage of reef-building corals are now higher in the GoP, a reversal of historic trends that may be due to ocean warming caused by climate change (Randall et al. 2020). Upwelling, which heretofore impeded reef growth, may now be ameliorating the harmful effects of extreme-temperature events associated with El Niño and global warming, by cooling the shallow waters of the GoP and increasing the availability of nutrients there (Karnauskas and Cohen 2012, Riegl et al. 2019, Storlazzi et al. 2020).

Coral recruitment was low throughout this study: individual recruits were recorded on only three BARs, all from Pedro González in the GoP. This result is in agreement with studies of

recruitment to artificial substrates (plexiglass and cement blocks) made in the GoP in the early 1970s (Birkeland 1977) and in the GoC in the mid to late 1980s (Eakin 1991). The coral skeleton from which the BARs were constructed in this study likely provided a more realistic representation of freshly available reef substrate, although a lack of cryptic recesses on freshly deployed BARs and the restriction of our analyses to upward-facing surfaces may have limited our assessment of settlement (Doropoulos et al. 2015). Regardless, the low recruitment in this study likely reflects poor large-scale connectivity of *Pocillopora* populations within the ETP, as well as between the ETP and the broader Indo-Pacific (Combosch and Vollmer 2011). Low coral recruitment has important ramifications for population recovery following disturbances, by limiting the potential for reestablishment by sexual reproduction. In the GoP, high grazing pressure and the rapid recruitment of heterotrophic invertebrates may further limit recovery to coral-dominated states, possibly resulting in habitat loss over time (Glynn 1994).

The fact that accretion-rates of CCA were not significantly different between gulfs (Appendix S1: Fig. S3, Table S5), whereas the accretion rates of heterotrophic suspension-feeding taxa were, supports the conclusion that productivity is likely the primary driver of the differences observed in this study. These results are surprising considering evidence of more favorable conditions for calcification by CCA in the relatively oligotrophic, lower pCO_2 GoC. Acidification, which is higher in the GoP, has been shown to lead to depressed calcification rates of CCA (Kuffner et al. 2008). Furthermore, elevated nutrients may favor fast-growing, fleshy macroalgae (Schaffelke and Klumpp 1998), yet there was no difference in the abundance of non-calcareous algae or the abundance of herbivorous grazers between gulfs in this study (see *External bioerosion*).

Although corals are the primary architects of reefs in the ETP and CCA is instrumental in binding and stabilizing reef-framework, the primary agents of carbonate accretion in this study were heterotrophic, suspension feeders such as barnacles and mollusks. These taxa were largely absent in the GoC, but abundant, yet patchily distributed, in the GoP. Exclusively heterotrophic, suspension-feeding fauna rapidly colonize dead-coral substrates in upwelling regions in the ETP (Wizemann et al. 2018). They are also relatively fast-growing, as evidenced by balanoid barnacles that have been observed to reach 15 mm in diameter in 56 d in the GoP (Birkeland 1977). This is in stark contrast to slower-growing corals, which produce more persistent bioherms.

In addition to total volume, the morphology, porosity, and crystalline structure of newly accreted calcium carbonate are important. These factors have implications for the structural integrity and permanence of the carbonate and, therefore, have ramifications for the reef-building potential of the benthos. Many of these processes likely influenced the composition and volume of the BARs over the short, two-year duration of this study. For example, broken shells and basal plates of dead barnacles were observed, indicating that erosion of structurally less-sound accretion had already occurred. Over longer periods, however, the loss, replacement, or overgrowth of the original *Porites* base with new calcareous formations could have more profound implications for rates of deposition and erosion. For example, feedback loops could occur whereby a more-ephemeral benthos would preclude the successful establishment of slower-growing and more-stable calcifiers. Dynamic benthic communities may increase the chance of successful settlement of opportunistic macroborers, further contributing to a potentially nonlinear decay in the physical and ecological structure of the reef.

These considerations are of particular importance when considering the responses observed in the GoP. Calcification rates, particularly by heterotrophic suspension-feeders, are likely not indicative of reef development, and instead they may contribute to less-stable forms of calcium carbonate, such as sediment and rubble, without providing the important biomass-supporting habitat characteristics of reef framework (Glynn et al. 1979, Enochs 2012, Reijmer et al. 2012). The composition of dredged carbonate sediments obtained from both gulfs indeed reflects a higher proportion of heterotrophic carbonate production, primarily barnacles, in the GoP (Schäfer et al. 2011, Reijmer et al. 2012). Reef-core data from the GoC reveal that carbonates derived from serpulids, vermetids, barnacles, and bryozoans, although present in the interstices of the reef framework, have not been important contributors to reef development there (Glynn and Macintyre 1977). Higher calcification rates recorded in the GoP may, therefore, be misleading in that they do not indicate greater potential for reef-framework construction; rather, they may point to a difference in the dominant calcifying assemblage and a greater potential for a shift in habitat structure, at least during the early successional stages following a disturbance.

External bioerosion

External bioerosion was the dominant process influencing BARs in this study, with average rates that were multiple times the magnitude of either accretion or macroboring. The relative importance of this process is not surprising given similar observations from the ETP (Alvarado et al. 2017) and reefs worldwide (Glynn and Manzello 2015). The external bioerosion rates recorded here (Appendix S1: Table S4) are within the range of carbonate-block-based measurements from the Great Barrier Reef (1,393 ± 1,065 $cm^3\ m^{-2}\ yr^{-1}$, over 1 yr [Tribollet et al. 2002]; 2,020 ± 2,073 $cm^3\ m^{-2}\ yr^{-1}$, over 3 yrs [Tribollet and Golubic 2005]; mean ± stdev of site averages) and French Polynesia (2,114 $cm^3\ m^{-2}\ yr^{-1}$, 2 yrs [Chazottes et al. 1995]; values

converted from kg using density of 1.05 g cm^{-3}). Values for external bioerosion in this study, however, exceed values reported for acidified sites in Papua New Guinea (412 ± 247 cm^3 m^{-2} yr^{-1}, Enochs et al. 2016), but are more than an order of magnitude less than reported from the Galápagos (21,300 ± 2,300 cm^3 m^{-2} yr^{-1}; Reaka-Kudla et al. 1996), which is considered to have some of the highest external bioerosion rates in the world (Alvarado et al. 2017).

Prior observations at two sites provide interesting comparison with our data, despite methodological differences. On the fore-reef slope of Uva Island, where BARs were deployed in this study, Eakin (1996) recorded external bioerosion rates (by *Diadema*, fish, and other motile taxa) of -2.32 kg m^{-2} yr^{-1}. On the lower seaward slope of Uva, Glynn (1988) calculated bioerosion rates by sea urchins of -0.14 to -0.28 and -3.47 to -10.40 kg m^{-2} yr^{-1} (units converted for comparison) before and after the 1982-1983 El Niño, respectively. At Saboga Island following that El Niño, urchin bioerosion was -4.64 kg m^{-2} yr^{-1} (Glynn 1988). Converting the volumes estimated from this study to mass using a mean initial substrate density of 1.05 g cm^{-3}, external bioerosion rates were -1.41 and -1.20 kg m^{-2} yr^{-1} at Uva and Saboga, respectively. Although these rates are lower than in earlier studies, methodological differences, including how erosion was measured and calculated, the duration of the studies, and the type of substrate considered (pocilloporid vs. poritid skeletons) likely account for the differences.

It is striking how similar external bioerosion rates were at Uva and Saboga; if the analysis had been limited to one site per gulf, it could have led to the erroneous conclusion that external bioerosion was the same in the GoP and GoC. In this study, however, higher rates of external bioerosion on average in the GoC ultimately drove the overall trend of greater net carbonate loss than in the GoP. This difference could have been influenced by fishing pressure, either directly through the targeted removal of grazing parrotfishes, or indirectly through the removal of

invertivore and piscivore fishes that control the populations of grazing taxa. Fishing is limited in the GoC, with many reefs protected within Coiba National Park, whereas the reefs studied in the GoP are in closer proximity to human habitation. Differences in the abundances of grazing taxa, however, were not detected between the two gulfs, which may be a result of high variability in a limited number of surveys. It is possible that the differences in carbonate loss due to grazing between the two gulfs were due to other factors. For instance, Smith (2008) observed that the bite-rate of the most abundant parrotfish observed in this study, *Scarus ghobban*, was significantly influenced by temperature. This led to fewer bites per minute, with presumably less substrate scarring, during the upwelling season in the GoP. Bite-rates were nearly twice as high during the non-upwelling season in the GoP and comparable to those recorded in the GoC throughout the year (Smith 2008). Interestingly, the opposite trend has been observed with respect to echinoid grazers, with higher external bioerosion rates in the GoP, driven in part by the larger body-sizes there (Glynn 1988, Eakin 1991). In that case, however, higher abundances of urchins in the GoC following the 1982–1983 El Niño led to higher total bioerosion in that gulf (Glynn 1988).

The relative contributions of parrotfish and urchins to overall bioerosion on the BARs is not possible to determine from the data collected in this study, but historically, relative contributions have been dynamic. In some circumstances—certain years, reef-zones, and regions—bioerosion by *Diadema* in the ETP has been even lower than by the non-echinoid infauna (Glynn 1988, Eakin 1991, 1996). Under other circumstances, strong recruitment or population redistribution have led to extremely elevated rates of echinoid bioerosion and strongly contributed to the loss of reef habitat (Glynn 1988, Eakin 1991, 1996, Glynn et al. 2020). That said, urchin densities reported herein are much lower than previously reported for Contadora and

Saboga, even considering the low abundances prior to the 1982–1983 El Niño (Glynn 1988). If site-specific erosion rates per individual *Diadema* (0.19 and 0.47 g individuals^{-1} day^{-1} at Uva and Saboga, respectively; Glynn 1988) are multiplied by the total densities of urchins we recorded at the same reefs, they account for only 2.2% and 6.0% of total recorded external bioerosion by mass at the two sites, respectively. The two most abundant parrotfish species observed in this study, *S. ghobban* and *S. rubroviolaceus*, use less-destructive scraping behaviors when foraging, but their populations have been known to reach densities resulting in erosion rates that exceed the majority of external bioerosion rates reported here (reviewed in Alvarado et al. 2017). Ultimately, it is impossible to make definitive conclusions concerning the processes contributing to the differences in external bioerosion rates between gulfs without a clearer understanding of the taxa involved, as their unique ecology will influence their impact on the persistence of reef framework.

Macroboring

Many macroboring taxa are heterotrophic, suspension-feeding animals, with prior studies indicating that the abundances (Rose and Risk 1985) and erosion rates (Achlatis et al. 2017, Prouty et al. 2017) of these species are stimulated by greater food availability, organic matter, and nutrients. For example, the abundance of excavating sponges appears to be strongly correlated with total nitrogen and ammonium levels in seawater (Ward-Paige et al. 2005), and greater infestation of macroborers (polychaetes, bivalves, sipunculid worms) have been recorded within productive, inshore regions of the Great Barrier Reef than offshore (Tribollet and Golubic 2005). Nutrients may act synergistically with other stressors such as acidification, leading to especially abundant bioeroding assemblages (DeCarlo et al. 2014, Prouty et al. 2017).

These factors, related to upwelling, likely contributed to the greater macroboring rates observed in the GoP. In contrast, an assessment of non-echinoid bioeroders on Uva and Saboga Islands in the 1980s based on change in the mass of pocilloporid framework over several days, revealed roughly equivalent erosion rates that were slightly greater in the GoC than in the GoP (mean = 8.60 and 8.14 kg m^{-2} yr^{-1}, GoC and GoP, respectively; Glynn 1988). Macroboring rates measured in the present study for those sites, converted from volume to mass based on mean substrate density, were more than an order of magnitude lower than reported by Glynn (1988): just 0.05 and 0.20 kg m^{-2} yr^{-1}, respectively. The measurements of bioerosion in the earlier study did incorporate the bioeroding activity of cryptic invertebrates such as crabs and gastropods, which may partially explain this discrepancy; however, other studies have documented similarly high macroboring at other locations in the ETP, particularly in areas that experience upwelling. Reaka-Kudla et al. (1996) deployed *Porites* blocks and high-density cathedral-limestone for a period of nearly 15 months in the southern Galápagos and calculated bioerosion rates to be 2.6 ± 0.1 kg m^{-2} yr^{-1} (mean ± SE) and 0.6 ± 0.1 kg m^{-2} yr^{-1} for the two types of calcium carbonate, respectively. Similar to this study, macroboring assemblages were dominated by lithophagine bivalves and polychaetes. Rates were still much higher than those reported here for the upwelling GoP (0.20 ± 0.12 kg m^{-2} yr^{-1}, converted as above). One potential explanation for the difference is that the blocks deployed in the Galápagos were thicker than those used here (4 vs. 1.5 cm), meaning that there was a greater amount of material that could be removed per unit surface area. Macroboring rates determined in the present study are, however, consistent with values reported from other regions of the world, including the relatively oligotrophic reef habitats off Lizard Island, Great Barrier Reef, where rates of macroboring ranged from 0.13 to 0.22 (Kiene and

Hutchings 1994) and 0.06 to 0.24 kg m^{-2} yr^{-1} (Kiene and Hutchings 1992), depending on location, exposure, and length of deployment.

The composition of the macroboring assemblage strongly depends on the amount of time the material is deployed. Changes in community composition and general patterns of succession are well documented (Davies and Hutchings 1983, Peyrot-Clausade et al. 1992, Kiene and Hutchings 1994). Many of these studies discuss the dominance of polychaetes during early successional stages and the later establishment of lithophagine bivalves. This pattern, however, may not hold true within upwelling regions in the ETP, including the Gulf of Papagayo in Costa Rica and the GoP, where colonization of endolithic bivalve mollusks may occur on the order of days to months (Kleemann 2013, Wizemann et al. 2018). The prevalence of these suspension-feeding faunas within the eutrophic GoP in this study, and their relative absence in the more oligotrophic GoC, drove the overall trends in macroboring. Their dominance among macroboring assemblages is corroborated by other observations in the ETP (Scott and Risk 1988, Reaka-Kudla et al. 1996, Cantera et al. 2003, Fonseca et al. 2006). Many of those studies also indicated the importance of annelid bioerosion, but annelids were only minor contributors to macrobioerosion in this study.

In contrast to boring bivalves, bioerosion by annelids was not significantly different between the two gulfs. Annelids have been documented to quickly colonize and infest carbonates within the ETP and rates of erosion were consistent across sites and reef zones (Cardona-Gutiérrez and Londoño-Cruz 2020). Prior work has shown these taxa to be responsive to CO_2, with higher erosion rates recorded closer to volcanically acidified reefs (Enochs et al. 2016); however, this pattern was not apparent in the intermittently acidified GoP. Polychaete food sources and feeding methodologies are diverse and complex, including carnivory, herbivory,

deposit-feeding, suspension-feeding, and combinations of these strategies (Fauchald and Jumars 1979). Dietary diversity or flexibility may explain why bioerosion rates were not detectably different between the two gulfs, whereas obligately suspension-feeding bivalves were significantly more abundant in the GoP.

There was a conspicuous absence of bioeroding sponges present within the BARs, which was surprising given their ubiquity on reefs worldwide and their well-documented presence within reef carbonates in the ETP (Alvarado et al. 2017). This observation, however, is not without precedent as a similar study in the Galápagos also observed a pronounced lack of bioeroding sponges relative to the Caribbean (Reaka-Kudla et al. 1996). In our study, it is possible that sparse and superficial colonization by sponges could have been mistaken for annelid boreholes during volumetric partitioning of the CT scans. It would be difficult, however, to mistake the clear gallery-like network of cavities created by endolithic poriferans for the tubular erosion of annelids. Relative to other regions, cryptic lifestyles are especially prevalent in the ETP, which is likely a consequence of strong grazing pressure and competition on epibenthic surfaces during settlement (Wulff 1997). Sponges that generally recruit to the dark undersides of coral colonies and into reef interstices would have been restricted to settling on only the upper surfaces of BARs due to the epoxied PVC bases that served as the attachment points and may therefore have been underrepresented as an artifact of our methodology. The structure of the *Porites* substrate may also have contributed to the low prevalence of bioeroding sponges in this study; the BARs were more homogeneous than the structurally complex and porous pocilloporid carbonates where many sponges grow in the ETP (Carballo et al. 2008, 2013). It is also possible that the composition of the grazing community influenced that of the macroborers, as high

prevalences of polychaetes vs. sponges have been observed in urchin and parrotfish-dominated areas, respectively (Carreiro-Silva and McClanahan 2012).

Lastly, it is important to note that the volumes of material removed or rates of macroboring may not tell the entire story with respect to the fate of the carbonate substrate. Bivalve boreholes, for example, increase porosity and can weaken the substrate, making it more prone to breakage (Scott and Risk 1988) or grazing (Rice et al. 2020). This type of internal structural alteration has been shown to influence larger-scale reef-framework morphology (Carballo et al. 2008). Although a certain degree of taphonomic alteration is critical for promoting biodiversity (Enochs and Manzello 2012) and biomass (Enochs 2012), these processes can lead to a loss of habitat and collapse in ecosystem function.

Microscopic processes (cementation and dissolution)

Bioerosion accretion replicates were constructed from material sourced from a single, remote location, so changes in the density of inconspicuously bored skeletal material are reflective of post-mortem alteration, rather than differences in coral calcification among the gulfs (Manzello 2010). Whereas the density of some individual BARs declined in this study (eight, exclusively from the GoP), the majority demonstrated an increase in density over the two-year deployment. One explanation for this result could be that macroboring or external bioerosion by grazers preferentially removed lower-density skeletal material, but this conclusion is not supported by the literature for macroboring taxa (Tribollet et al. 2002) and seems unlikely for grazers given the homogeneous nature of the *Porites* skeletons. Instead, it is possible that precipitation of submarine cements (Perry and Hepburn 2008) exceeded dissolution, driving the net increase in density in these areas of the skeleton. This is surprising considering the poorly cemented nature of reefs within the ETP relative to other parts of the world (Manzello et al.

2008). The greater increase in density of BARs from the GoC relative to the GoP, however, is supported by the prevalence of intraskeletal cementation present within reef-framework substrates, which is nearly two times higher in the GoC compared with the GoP (Manzello et al. 2008).

Although cementation was likely the dominant microscopic process affecting the BARs, it is probable that dissolution also occurred, driven primarily by a phototrophic assemblage of microborers (cyanobacteria and chlorophyte algae), as well as marine fungi. A previous study, which adopted the same approach of CT-based densitometry of intact coral skeletons, recorded a net decline in density, which was interpreted as dissolution due to abiotic and microboring processes in a naturally CO_2-enriched environment (Enochs et al. 2016). Microborers have been observed to colonize freshly available coral substrate rapidly, within a period of less than one month (Wizemann et al. 2018). Manipulative experiments have revealed that microboring rates are accelerated by acidification (Tribollet et al. 2009) as well as nutrients and organic matter, depending on the trophic requirements of the species involved (Carreiro-Silva et al. 2009). Differential rates of microbioerosion between gulfs could have contributed to the overall trends in BAR density, with the relatively eutrophic and acidified conditions in the GoP increasing microboring and decreasing the overall density despite a net positive increase. Correlative field-based assessments, although similar to the approach used here, are not as clear as experiments with respect to OA and nutrient enhancement of microborers. Enochs et al. (2016) detected no significant differences in microboring along a CO_2 gradient associated with a volcanically acidified coral reef. Tribollet (2008) actually observed higher microboring rates at offshore, oligotrophic sites, owing to co-occurring factors such as inshore turbidity and sedimentation. Direct identification of the causative agents or mechanisms behind these patterns is beyond the

scope of this study, and further studies are needed on this functional group of bioeroders, particularly in the ETP (Alvarado et al. 2017).

Additional functional-group interactions

Interactions between functional groups accreting to and eroding dead-coral substrate are numerous (Chazottes et al. 1995). For example, both microboring and macroboring can contribute to higher grazing rates by attracting grazers or weakening substrate (Chazottes et al. 1995, Rice et al. 2020). Macroboring may also contribute to colony-fracture from physical disturbance by weakening the skeleton (Tunnicliffe 1979, Scott and Risk 1988), as well as by attracting invertivorous fishes that are capable of breaking carbonate substrate while foraging (Guzman 1988). Due to the resulting separation and removal of surface material, this initial superficial boring would have been quantified as external bioerosion in this study, making the importance of such relationships difficult to discern. In contrast with previous observations, we found that external bioerosion was higher in the GoC, where macroboring was lower and substrate density was higher, presumably correlating with less microbioerosion. One possible explanation for this disparity is that grazing fishes, which may obtain nutrients from eating microborers, are preferentially removing the upper layers of substrate where this community resides (Chazottes et al. 1995). Therefore, although microboring may have been active, what was detected in the post-deployment CT scans was the material that had remained unbored and unremoved. This hypothesis, however, does not fully explain the net positive density changes in the GoC.

Despite the overwhelming importance of external bioerosion between the gulfs, it is interesting that the vectors for both grazer abundances and external bioerosion show up as orthogonal to the clear separation of the gulfs in the PCA plot. This suggests that differences in

external bioerosion were not as closely correlated with differentiation between gulfs as heterotrophic calcification. Just as interesting is the strong negative correlation between external bioerosion and CCA calcification in the ordination of the BARs. The relationship of these vectors could indicate that grazing removed CCA or that the surfaces of the BARs were removed before CCA was able to become dominant. This pattern is also interesting within the context of nutrients as outlined in the relative-dominance model proposed by Littler and Littler (1985). According to this model, coralline algae should be dominant in areas of high herbivory and high nutrients. “High” is of course subjective, and grazing is a feeding strategy that is not exclusively erosional in nature. Data herein, however, suggest that abundances of grazers were similar between the gulfs despite differences in nutrient regimes, although grazing pressure could theoretically be higher in the GoC due to larger body sizes and higher frequencies of feeding. With stronger upwelling and eutrophication in the GoP than in the GoC, the model would predict dominance by CCA and corals, respectively (Littler and Littler 1985); however, epibenthic surfaces were primarily dominated by algae and bare substrate, with CCA being the third-most-abundant category of cover and no clearly discernible difference between gulfs. Furthermore, coral coverage is presently higher in the GoP (Randall et al. 2020).

Implications for reef-framework persistence in the ETP and worldwide

In many ways the ETP has served as a harbinger of the changes to reef form and function occurring worldwide today. The sensitivity of response of reefs in the ETP has been due in large part to the highly dynamic and marginal environment, where extremes in temperature and CO_2 have provided insights into how corals will respond to global warming and acidification (Glynn 1984, Glynn and D'Croz 1990, Manzello et al. 2008). The fates of the BARs in this study extend beyond framework-construction by living corals to the multiphyletic consortium that influences

the persistence of dead carbonates and reef-framework habitats. That consortium has profound implications for reef ecosystems worldwide, which are increasingly marked by mass-bleaching events and widespread coral mortality that has led to precipitous declines in coral cover and an increasing importance of erosive processes.

The net erosion of BARs in both gulfs does not bode well for reef-framework persistence in the region. Particularly high external bioerosion relative to accretion drove this trend across both gulfs, resulting in net declines in both volume and mass. As discussed earlier, coral recruitment was low and, therefore, the fate of BARs provides insights into the likely trajectories of reef-framework following a major coral mortality event. Such events are not without precedent in the ETP, an area marked by dramatic fluctuations in coral abundance. In the Galápagos Islands, for example, a single, extreme-temperature event, the 1982–1983 El Niño, led to widespread coral bleaching and mortality (Glynn 1994). High grazing pressure and bioerosion from urchins led to the loss of suitable substrate and the inhibition of settlement, precluding the recovery of coral populations. At Uva Island in the GoC, the same El Niño event resulted in coral mortality and the enhancement of bioerosion, shifting the reefs from net accretion to net erosion (Eakin 1996). In the years since, however, coral cover has increased greatly at Uva Island, demonstrating a remarkable degree of resilience (Glynn et al. 2014), whereas at many sites in the Galápagos coral populations are still absent today.

The Galápagos experience upwelling, high CO_2, and elevated productivity like the GoP. Upwelling likely contributes to more dynamic calcification and bioerosion, as evident from the higher rates of heterotrophic, suspension-feeding calcification and macroboring measured in the GoP than the GoC. The persistence of coral-reef carbonates in these environments may be more tenuous and more prone to collapse (Toth et al. 2012, Toth et al. 2015), even as these same

hydrographic conditions provide thermal refugia for scleractinian corals and permit higher growth rates in a warming ocean (Randall et al. 2020). The decoupling of coral growth rates and reef-framework persistence has been documented in other eutrophic environments throughout the world, driven in part by bioerosion (Hallock 1988, Edinger et al. 2000).

Considering the ecological diminution of coral calcification, the results of this study suggest that dead-carbonate materials are especially susceptible to external bioerosion. In areas of active and abundant herbivory, as in remote regions and within marine reserves with restricted fishing, herbivorous parrotfish and urchins may be the most important factors influencing habitat longevity (Bruno et al. 2019). Active grazing has long been considered critical to proper reef function, removing algae that can compete for space with corals and inhibit coral recruitment (McCook 1999, McCook et al. 2001). The impact on ecosystem health is of course more nuanced. Counterintuitively, if corals are rendered ecologically irrelevant, active grazing will accelerate the loss of reef habitat and the ecosystem services that coral reefs provide.

Acknowledgements

We thank Northeastern University's Three Seas Program and the students of Three Seas classes XXXII–XXXV for help with data collection. The staffs at the Smithsonian Tropical Research Institute and the Liquid Jungle Lab, G. Schuttke of Coral Dreams, B. Steffel, A. Zamora-Duran, and D. Kline provided field support. Field work was conducted under research permits from the Ministerio de Ambiente, Republica de Panamá. V. Brandtneris, P. Fong, W. McGillis, A. Palacio, and T. Smith assisted with instrument deployment and recovery. N. Besemer helped with the analysis of CT scans. J. Crawford, B. Precht, and C. Kelble provided assistance during manuscript preparation. Analytical instrumentation was acquired with funding from NOAA, with support from the Coral Reef Conservation Program (CRCP) and the Ocean Acidification

Program (OAP). This research was funded by U.S. National Science Foundation grant OCE-1535007 to R.B. Aronson and L.T. Toth, OCE-1535203 to J.J. Leichter, and OCE-1447341 to P. Fong. Any use of trade, firm, or product names is for descriptive purposes only and does not imply endorsement by the U.S. Government. This is contribution no. 237 from the Institute for Global Ecology at the Florida Institute of Technology.

Literature Cited

Achlatis, M., R. M. van der Zande, C. H. L. Schönberg, J. K. H. Fang, O. Hoegh-Guldberg, and S. Dove. 2017. Sponge bioerosion on changing reefs: ocean warming poses physiological constraints to the success of a photosymbiotic excavating sponge. Scientific Reports **7**:10705.

Alvarado, J. J., B. Grassian, J. R. Cantera-Kintz, J. L. Carballo, and E. Londoño-Cruz. 2017. Coral Reef Bioerosion in the Eastern Tropical Pacific. Pages 369-403 *in* P. W. Glynn, D. M. Manzello, and I. C. Enochs, editors. Coral Reefs of the Eastern Tropical Pacific.

Alvarez-Filip, L., N. K. Dulvy, J. A. Gill, I. M. Cote, and A. R. Watkinson. 2009. Flattening of Caribbean coral reefs: region-wide declines in architectural complexity. Proceedings of the Royal Society B **276**:3019-3025.

Baker, A. C., P. W. Glynn, and B. Riegl. 2008. Climate change and coral reef bleaching: An ecological assessment of long-term impacts, recovery trends and future outlook. Estuarine, Coastal and Shelf Science **80**:435-471.

Beijbom, O., P. J. Edmunds, C. Roelfsema, J. Smith, D. I. Kline, B. P. Neal, M. J. Dunlap, V. Moriarty, T. Y. Fan, C. J. Tan, S. Chan, T. Treibitz, A. Gamst, B. G. Mitchell, and D. Kriegman. 2015. Towards automated annotation of benthic survey images: Variability of human experts and operational modes of automation. PLoS One **10**:e0130312.

Birkeland, C. 1977. The importance of rate of biomass accumulation in early successional stages of benthic communities to the survival of coral recruits. Proceedings of the 3rd International Coral Reef Symposium:15-21.

Bruno, J. F., I. M. Côté, and L. T. Toth. 2019. Climate change, coral loss, and the curious case of the parrotfish paradigm: Why don't marine protected areas Iimprove reef resilience? Annual Review of Marine Science **11**:307-334.

Cantera, J. R., C. Orozco, E. Londoño-Cruz, and G. Toro-Farmer. 2003. Abundance and distribution patterns of infaunal associates and macroborers of the branched coral (*Pocillopora damicornis*) in Gorgona Island (Eastern Tropical Pacific). Bulletin of Marine Science **72**:207-219.

Carballo, J. L., E. Bautista, H. Nava, J. A. Cruz-Barraza, and J. A. Chávez. 2013. Boring sponges, an increasing threat for coral reefs affected by bleaching events. Ecol Evol **3**:872-886.

Carballo, J. L., E. Bautista-Guerrero, and G. E. Leyte-Morales. 2008. Boring sponges and the modeling of coral reefs in the east Pacific Ocean. Marine Ecology Progress Series **356**:113-122.

Cardona-Gutiérrez, M. F., and E. Londoño-Cruz. 2020. Boring worms (Sipuncula and Annelida: Polychaeta): their early impact on Eastern Tropical Pacific coral reefs. Marine Ecology Progress Series **641**:101-110.

Carreiro-Silva, M., and T. R. McClanahan. 2012. Macrobioerosion of dead branching *Porites*, 4 and 6 years after coral mass mortality. Marine Ecology Progress Series **458**:103-122.

Carreiro-Silva, M., T. R. McClanahan, and W. E. Kiene. 2009. Effects of inorganic nutrients and organic matter on microbial euendolithic community composition and microbioerosion rates. Marine Ecology Progress Series **392**:1-15.

Chan, N. C., and S. R. Connolly. 2013. Sensitivity of coral calcification to ocean acidification: a meta-analysis. Global Change Biology **19**:282-290.

Chaves-Fonnegra, A., B. Riegl, S. Zea, J. V. Lopez, T. Smith, M. Brandt, and D. S. Gilliam. 2018. Bleaching events regulate shifts from corals to excavating sponges in algae-dominated reefs. Glob Chang Biol **24**:773-785.

Chazottes, V., T. L. Campion-Alsumard, and M. Peyrot-Clausade. 1995. Bioerosion rates on coral reefs: interactions between macroborers, microborers and grazers (Moorea, French Polynesia). Palaeogeography, Palaeoclimatology, Palaeoecology **113**:189-198.

Combosch, D. J., and S. V. Vollmer. 2011. Population genetics of an ecosystem-defining reef coral *Pocillopora damicornis* in the Tropical Eastern Pacific. PLoS One **6**:e21200.

Darling, E. S., and I. M. Côté. 2008. Quantifying the evidence for ecological synergies. Ecological Letters **11**:1278-1286.

Davies, P. J., and P. A. Hutchings. 1983. Initial colonization, erosion and accretion on coral substrate: Experimental results, Lizard Island, Great Barrier Reef. Coral Reefs **2**:27-35.

D'Croz, L., and A. O'Dea. 2007. Variability in upwelling along the Pacific shelf of Panama and implications for the distribution of nutrients and chlorophyll. Estuarine, Coastal and Shelf Science **73**:325-340.

De'ath, G., K. E. Fabricius, H. Sweatman, and M. Puotinen. 2012. The 27-year decline of coral cover on the Great Barrier Reef and its causes. Proceedings of the National Academy of Sciences **109**:17995-17999.

DeCarlo, T. M., A. L. Cohen, H. C. Barkley, Q. Cobban, C. Young, K. E. Shamberger, R. E. Brainard, and Y. Golbuu. 2014. Coral macrobioerosion is accelerated by ocean acidification and nutrients. Geology **43**:7-10.

Delignette-Muller, M., and C. Dutang. 2015. fitdistrplus: An R Package for Fitting Distributions. Journal of Statistical Software **6**:1-34.

Doropoulos, C., G. Roff, Y.-M. Bozec, M. Zupan, J. Werminghausen, and P. J. Mumby. 2015. Characterising the ecological trade-offs throughout the early ontogeny of coral recruitment. Ecological Monographs.

Eakin, C. M. 1991. The damselfish-algal lawn symbiosis and its influence on the bioerosion of an El Niño impacted coral reef, Uva Island, Pacific Panama. University of Miami.

Eakin, C. M. 1996. Where have all the carbonates gone? A model comparison of calcium carbonate budgets before and after the 1982-1983 EI Niño at Uva Island in the eastern Pacific. Coral Reefs **15**:109-119.

Edinger, E. N., G. V. Limmon, J. Jompa, W. Widjatmoko, J. M. Heikoop, and M. J. Risk. 2000. Normal Coral Growth Rates on Dying Reefs: Are Coral Growth Rates Good Indicators of Reef Health? Marine Pollution Bulletin **40**:404-425.

Enochs, I. C. 2012. Motile cryptofauna associated with live and dead coral substrates: implications for coral mortality and framework erosion. Marine Biology **159**:709-722.

Enochs, I., D. Manzello, E. Donham, G. Kolodziej, R. Okano, L. Johnston, C. Young, J. Iguel, C. Edwards, M. Fox, L. Valentino, S. Johnson, D. Benavente, S. Clark, R. Carlton, T. Burton, Y. Eynaud, and N. Price. 2015. Shift from coral to macroalgae dominance on a volcanically acidified reef. Nature Climate Change **5**:1083-1089.

Enochs, I. C., et al. 2021. Upwelling and the persistence of coral-reef frameworks in the eastern tropical Pacific, carbonate data, chlorophyll data, and others from 2015-08-21 to 2019-04-05 (NCEI Accession 0239049). NOAA National Centers for Environmental Information. Dataset. https://www.ncei.noaa.gov/archive/accession/0239049

Enochs, I., and P. W. Glynn. 2016. Trophodynamics of eastern Pacific coral reefs.*in* P. W. Glynn, D. Manzello, and I. Enochs, editors. Coral reefs of the eastern tropical Pacific: Persistence and loss in a dynamic environment. Springer.

Enochs, I. C., and D. P. Manzello. 2012. Species richness of motile cryptofauna across a gradient of reef framework erosion. Coral Reefs **31**:653-661.

Enochs, I. C., D. P. Manzello, G. Kolodziej, S. H. Noonan, L. Valentino, and K. E. Fabricius. 2016. Enhanced macroboring and depressed calcification drive net dissolution at high-CO_2 coral reefs. Proceedings of the Royal Society B **283**:20161742.

Fabricius, K. E., C. Langdon, S. Uthicke, C. Humphrey, S. Noonan, G. De'ath, R. Okazaki, N. Muehllehner, M. S. Glas, and J. M. Lough. 2011. Losers and winners in coral reefs acclimatized to elevated carbon dioxide concentrations. Nature Climate Change **1**:165-169.

Fauchald, K., and P. A. Jumars. 1979. The diet of worms: A study of polychaete feeding guilds. Marine Biology and Oceanography Annual Review **17**:193-284.

Fonseca, A. C., H. K. Dean, and J. Cortés. 2006. Non-colonial coral macro-borers as indicators of coral reef status in the south Pacific of Costa Rica. Revista de Biologia Tropical **54**:101-115.

Gardner, T. A., I. M. Cöté, J. A. Gill, A. Grant, and A. R. Watkinson. 2003. Long-term region-wide declines in Caribbean corals. Science **301**:958-960.

Glynn, P. W. 1984. Widespread coral mortality and the 1982-83 El Niño warming event. Environmental Conservation **11**:133-146.

Glynn, P. W. 1988. El Niño warming, coral mortality and reef framework destruction by echinoid bioerosion in the eastern Pacific. Galaxea **7**:129-160.

Glynn, P. W. 1994. State of coral reefs in the Galápagos Islands: Natural vs anthropogenic impacts. Marine Pollution Bulletin **29**:131-140.

Glynn, P. W., and L. D'Croz. 1990. Experimental evidence for high temperature stress as the cause of El Niño-coincident coral mortality. Coral Reefs **8**:181-191.

Glynn, P. W., I. C. Enochs, J. A. Afflerbach, V. W. Brandtneris, and J. E. Serafy. 2014. Eastern Pacific reef fish responses to coral recovery following El Niño disturbances. Marine Ecology Progress Series **495**:233-247.

Glynn, P. J., P. W. Glynn, J. L. Maté, and B. Riegl. 2020. Agent-based model of Eastern Pacific damselfish and sea urchin interactions shows increased coral reef erosion under post-ENSO conditions. Ecological Modelling **423**.

Glynn, P. W., and I. G. Macintyre. 1977. Growth rate and age of coral reefs on the Pacific coast of Panama. Proceedings of the Third International Coral Reef Symposium:251-259.

Glynn, P. W., and D. P. Manzello. 2015. Bioerosion and coral reef growth: A dynamic balance. Pages 69-97 *in* C. Birkeland, editor. Coral reefs in the Anthropocene. Springer, Dordrecht.

Glynn, P. W., and J. L. Maté. 1997. Field guide to the Pacific coral reefs of Panamá. Proceedings of the 8th International Coral Reef Symposium **1**:145-166.

Glynn, P. W., and R. H. Stewart. 1973. Distribution of coral reefs in the Pearl Islands (Gulf of Panamá) in relation to thermal conditions. Limnology and Oceanography **18**:367-379.

Glynn, P. W., G. M. Wellington, and C. Birkeland. 1979. Coral reef growth in the Galápagos: limitation by sea urchins. Science **203**:47-49.

Grolemund, G., and H. Wickham. 2011. Dates and times made easy with lubridate. Journal of Statistical Software **40**:1-25.

Guzman, H. M. 1988. Distribución y abundancia de organismos coralívoros en los arrecifes coralinos de la Isla del Caño, Costa Rica. Revista de Biologia Tropical **36**:191-207.

Hallock, P. 1988. The role of nutrient availability in bioerosion: Consequences to carbonate buildups. Palaeogeography Palaeoclimatology Palaeoecology **63**:275-291.

Hu, C., Z. Lee, and B. Franz. 2012. Chlorophyll *a* algorithms for oligotrophic oceans: A novel approach based on three-band reflectance difference. Journal of Geophysical Research: Oceans **117**:C01011.

Hutchings, P. 2008. Role of polychaetes in bioerosion of coral substrates. Pages 249-264 *in* M. Wisshak and L. Tapanila, editors. Current Developments in Bioerosion. Springer Berlin Heidelberg, Berlin, Heidelberg.

Inoue, S., H. Kayanne, S. Yamamoto, and H. Kurihara. 2013. Spatial community shift from hard to soft corals in acidified water. Nature Climate Change **3**:683-687.

Karnauskas, K. B., and A. L. Cohen. 2012. Equatorial refuge amid tropical warming. Nature Climate Change **2**:530-534.

Kiene, W. E., and P. Hutchings. 1992. Long-term bioerosion of experimental coral substrates from Lizard Island, Great Barrier Reef. Proceedings of the 7th International Coral Reef Symposium, Guam **1**:397-403.

Kiene, W. E., and P. A. Hutchings. 1994. Bioerosion experiments at Lizard Island, Great-Barrier-Reef. Coral Reefs **13**:91-98.

Kleemann, K. 2013. Fast and massive settlement of boring bivalves on coral slabs at Taboga Islands, Eastern Pacific, Panama. Bollettino Malacologico **49**:104-113.

Kuffner, I. B., A. J. Andersson, P. L. Jokiel, K. S. Rodgers, and F. T. Mackenzie. 2008. Decreased abundance of crustose coralline algae due to ocean acidification. Nature Geoscience **1**:114-117.

Lirman, D., S. Schopmeyer, D. Manzello, L. J. Gramer, W. F. Precht, F. Muller-Karger, K. Banks, B. Barnes, E. Bartels, A. Bourque, J. Byrne, S. Donahue, J. Duquesnel, L. Fisher, D. Gilliam, J. Hendee, M. Johnson, K. Maxwell, E. McDevitt, J. Monty, D. Rueda, R. Ruzicka, and S. Thanner. 2011. Severe 2010 cold-water event caused unprecedented mortality to corals of the Florida reef tract and reversed previous survivorship patterns. PLoS One **6**:e23047.

Littler, M., and D. Littler. 1984. A relative-dominance model for biotic reefs. Proceedings of the Joint Meeting of the Atlantic Reef Committee Society of Reef Studies, Miami, Florida.

Manzello, D. P. 2010. Coral growth with thermal stress and ocean acidification: lessons from the eastern tropical Pacific. Coral Reefs **29**:749-758.

Manzello, D. P., J. A. Kleypas, D. A. Budd, C. M. Eakin, P. W. Glynn, and C. Langdon. 2008. Poorly cemented coral reefs of the eastern tropical Pacific: possible insights into reef development in a high-CO_2 world. Proceedings of the National Academy of Sciences **105**:10450-10455.

McCook, L. J. 1999. Macroalgae, nutrients and phase shifts on coral reefs scientific issues and management consequences for the Great Barrier. Coral Reefs **18**:357-367.

McCook, L., J. Jompa, and G. Diaz-Pulido. 2001. Competition between corals and algae on coral reefs: a review of evidence and mechanisms. Coral Reefs **19**:400-417.

Moberg, F., and C. Folke. 1999. Ecological goods and services of coral reef ecosystems. Ecological Economics **29**:215-233.

Oksanen, J., F. G. Blanchet, M. Friendly, R. Kindt, P. Legendre, D. McGlinn, P. R. Minchin, R. B. O'Hara, G. L. Simpson, P. Solymos, M. H. H. Stevens, E. Szoecs, and H. Wagner. 2019. vegan: Community Ecology Package.

Perry, C. T., L. Alvarez-Filip, N. A. J. Graham, P. J. Mumby, S. K. Wilson, P. S. Kench, D. P. Manzello, K. M. Morgan, A. B. A. Slangen, D. P. Thomson, F. Januchowski-Hartley, S. G. Smithers, R. S. Steneck, R. Carlton, E. N. Edinger, I. C. Enochs, N. Estrada-Saldívar, M. D. E. Haywood, G. Kolodziej, G. N. Murphy, E. Pérez-Cervantes, A. Suchley, L. Valentino, R. Boenish, M. Wilson, and C. Macdonald. 2018. Loss of coral reef growth capacity to track future increases in sea level. Nature **558**:396-400.

Perry, C. T., and L. J. Hepburn. 2008. Syn-depositional alteration of coral reef framework through bioerosion, encrustation and cementation: Taphonomic signatures of reef accretion and reef depositional events. Earth-Science Reviews **86**:106-144.

Peyrot-Clausade, M., P. Hutchings, and G. Richard. 1992. Temporal Variations of Macroborers in Massive Porites-Lobata on Moorea, French-Polynesia. Coral Reefs **11**:161-166.

Prouty, N. G., A. Cohen, K. K. Yates, C. D. Storlazzi, P. W. Swarzenski, and D. White. 2017. Vulnerability of coral reefs to bioerosion from land-based sources of pollution. Journal of Geophysical Research: Oceans **122**:9319-9331.

RCore Team. 2008. R: A language and environment for statistical computing. R Foundation for Statistical Computing, Vienna, Austria.

Randall, C. J., L. T. Toth, J. J. Leichter, J. L. Maté, and R. B. Aronson. 2020. Upwelling buffers climate change impacts on coral reefs of the eastern tropical Pacific. Ecology **101**:e02918.

Reaka-Kudla, M. L., J. S. Feingold, and P. W. Glynn. 1996. Experimental studies of rapid bioerosion of coral reefs in the Galápagos Islands. Coral Reefs **15**:101-107.

Reijmer, J. J. G., T. Bauch, and P. Schäfer. 2012. Carbonate facies patterns in surface sediments of upwelling and non-upwelling shelf environments (Panama, East Pacific). Sedimentology **59**:32-56.

Rice, M. M., R. L. Maher, A. M. S. Correa, H. V. Moeller, N. P. Lemoine, A. A. Shantz, D. E. Burkepile, and N. J. Silbiger. 2020. Macroborer presence on corals increases with nutrient input and promotes parrotfish bioerosion. Coral Reefs **39**:409-418.

Riegl, B., P. W. Glynn, S. Banks, I. Keith, F. Rivera, M. Vera-Zambrano, C. D'Angelo, and J. Wiedenmann. 2019. Heat attenuation and nutrient delivery by localized upwelling avoided coral bleaching mortality in northern Galapagos during 2015/2016 ENSO. Coral Reefs **38**:773-785.

Rose, C. S., and M. J. Risk. 1985. Increase in *Cliona delitrix* infestation of *Montastrea cavernosa* heads on an organically polluted portion of the Grand Cayman fringing reef. Marine Ecology **6**:345-363.

RStudio Team. 2015. RStudio: Integrated development for R. RStudio, Inc., Boston, MA.

Schäfer, P., H. Fortunato, B. Bader, V. Liebetrau, T. Bauch, and J. J. G. Reijmer. 2011. Growth rates and carbonate production by coralline red algae in upwelling and non-upwelling settings along the Pacific coast of Panama. Palaios **26**:420-432.

Schaffelke, B., and D. Klumpp. 1998. Short-term nutrient pulses enhance growth and photosynthesis of the coral reef macroalga *Sargassum baccularia*. Marine Ecology Progress Series **170**:95-105.

Scott, P., and M. J. Risk. 1988. The effect of *Lithophaga* (Bivalvia Mytilidae) boreholes on the strength of the coral *Porites lobata.* Coral Reefs **7**:145-151.

Silbiger, N. J., Ò. Guadayol, F. I. M. Thomas, and M. J. Donahue. 2014. Reefs shift from net accretion to net erosion along a natural environmental gradient. Marine Ecology Progress Series **515**:33-44.

Smith, T. B. 2008. Temperature effects on herbivory for an Indo-Pacific parrotfish in Panamá: implications for coral–algal competition. Coral Reefs **27**:397-405.

Storlazzi, C. D., O. M. Cheriton, R. van Hooidonk, Z. Zhao, and R. Brainard. 2020. Internal tides can provide thermal refugia that will buffer some coral reefs from future global warming. Sci Rep **10**:13435.

Tomascik, T., and F. Sander. 1985. Effects of eutrophication on reef-building corals: 1. Growth-rate of the reef-building coral *Montastrea annularis*. Marine Biology **87**:143-155.

Toth, L. T., R. B. Aronson, K. M. Cobb, H. Cheng, R. L. Edwards, P. R. Grothe, and H. R. Sayani. 2015. Climatic and biotic thresholds of coral-reef shutdown. Nature Climate Change **5**:369-374.

Toth, L. T., R. B. Aronson, S. V. Vollmer, J. W. Hobbs, D. H. Urrego, H. Cheng, I. C. Enochs, D. J. Combosch, R. van Woesik, and I. G. Macintyre. 2012. ENSO drove 2500-year collapse of eastern Pacific coral reefs. Science **337**:81-84.

Tribollet, A. 2008. Dissolution of dead corals by euendolithic microorganisms across the northern Great Barrier Reef (Australia). Microbial Ecology **55**:569-580.

Tribollet, A., G. Decherf, P. A. Hutchings, and M. Peyrot-Clausade. 2002. Large-scale spatial variability in bioerosion of experimental coral substrates on the Great Barrier Reef (Australia): importance of microborers. Coral Reefs **21**:424-432.

Tribollet, A., C. Godinot, M. Atkinson, and C. Langdon. 2009. Effects of elevated pCO_2 on dissolution of coral carbonates by microbial euendoliths. Global Biogeochemical Cycles **23**:1-7.

Tribollet, A., and S. Golubic. 2005. Cross-shelf differences in the pattern and pace of bioerosion of experimental carbonate substrates exposed for 3 years on the northern Great Barrier Reef, Australia. Coral Reefs **24**:422-434.

Tunnicliffe, V. 1979. The role of boring sponges in coral fracture. Colloques Internationeaux du CNRS **291**:309-315.

Ward-Paige, C. A., M. J. Risk, O. A. Sherwood, and W. C. Jaap. 2005. Clionid sponge surveys on the Florida Reef Tract suggest land-based nutrient inputs. Marine Pollution Bulletin **51**:570-579.

Wickham, H. 2011. The split-apply-combine strategy for data analysis. Journal of Statistical Software **40**:1-29.

Wickham, H. 2016. ggplot2: Elegant Graphics for Data Analysis. Springer-Verlag, New York.

Wizemann, A., S. D. Nandini, I. Stuhldreier, C. Sanchez-Noguera, M. Wisshak, H. Westphal, T. Rixen, C. Wild, and C. E. Reymond. 2018. Rapid bioerosion in a tropical upwelling coral reef. PLoS One **13**:e0202887.

Wulff, J. L. 1997. Causes and consequences of differences in sponge diversity and abundance between the Caribbean and eastern Pacific Panama. Proceedings of the 8th International Coral Reef Symposium **2**:1377-1382.

Yates, K. K., D. G. Zawada, N. A. Smiley, and G. Tiling-Range. 2017. Divergence of seafloor elevation and sea level rise in coral reef ecosystems. Biogeosciences **14**:1739-1772.

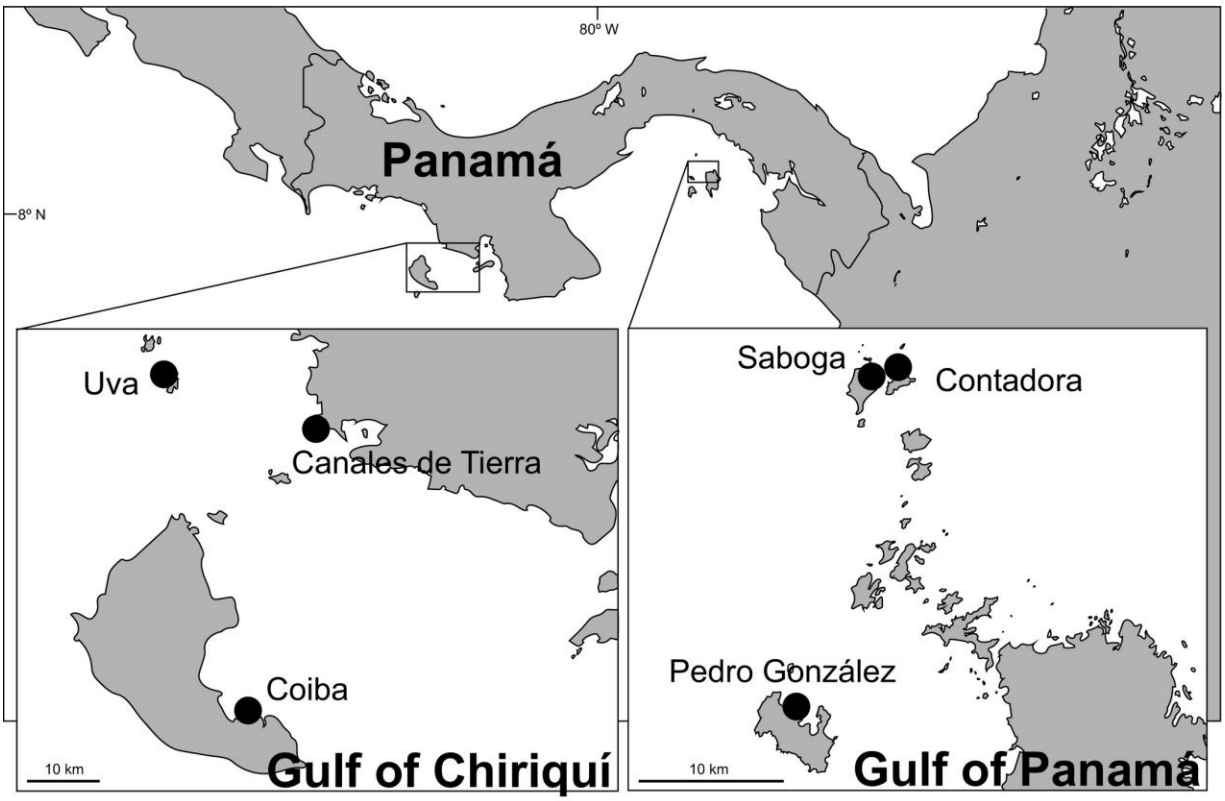

Figure 1. Location of the three study sites in each of two gulfs on the Pacific coast of Panamá. Scale bars in the inset of each gulf are 10 km.

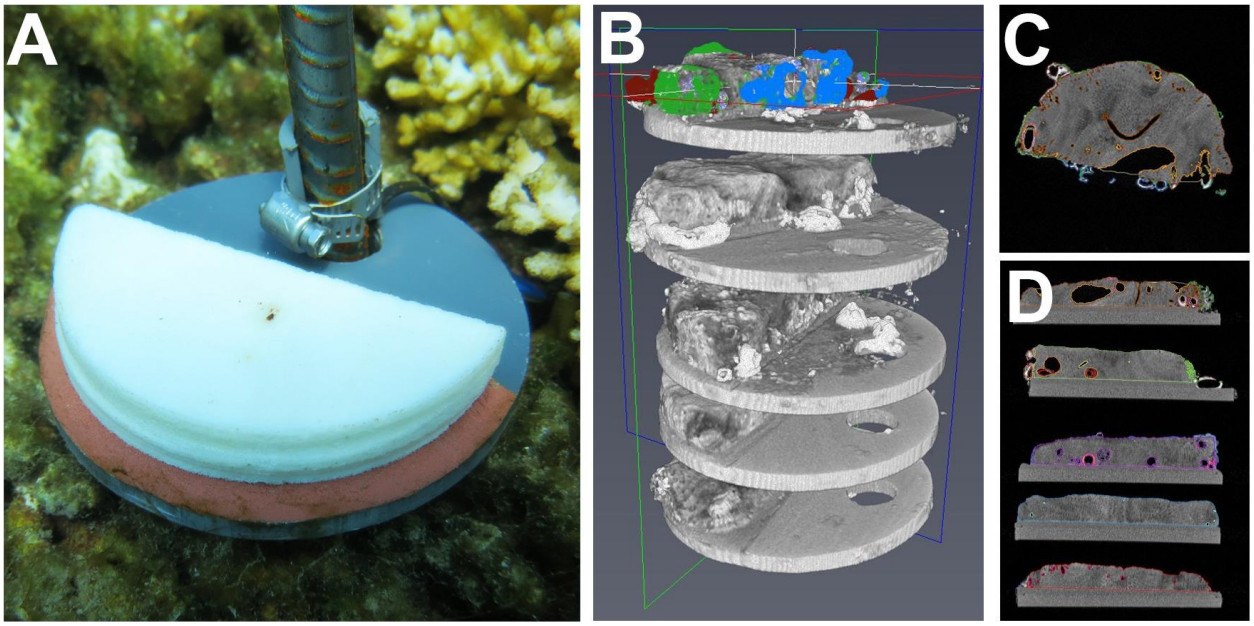

Figure 2. (A) Bioerosion accretion replicate (BAR) freshly installed on a pocilloporid reef using rebar and a hose clamp. A CT scan of five BARs including (B) three-dimensional reconstruction, (C) a two-dimensional axial slice, and (D) a two-dimensional sagittal slice. Colors represent volumetric quantification of different carbonate-altering functional groups. Photo in A taken by L. Toth, US Geological survey. Images in B-D generated at the Atlantic Oceanographic and Meteorological Laboratory, NOAA.

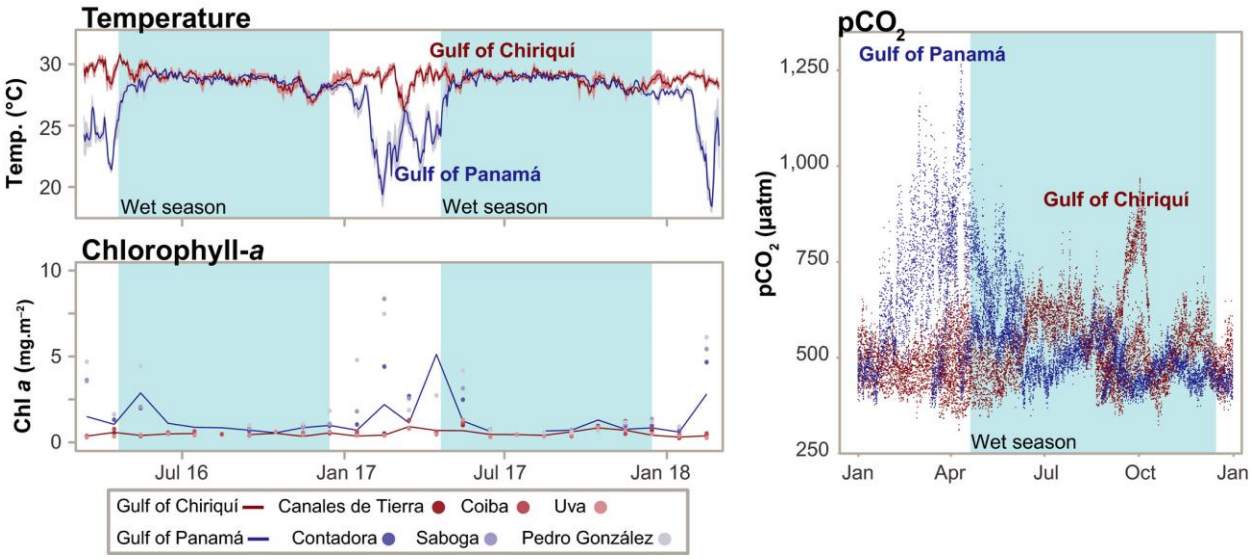

Figure 3. Temperature (Temp.), chlorophyll *a* (Chl *a*), and pCO_2 within the Gulfs of Panamá (blue) and Chiriquí (red). The wet season is denoted by light-blue shading. Temperature data are the means (solid line) and standard deviations (shading) of three sites within each gulf. Chlorophyll *a* data are presented for each site (dots) as well as averaged across the entire extent of each gulf (lines).

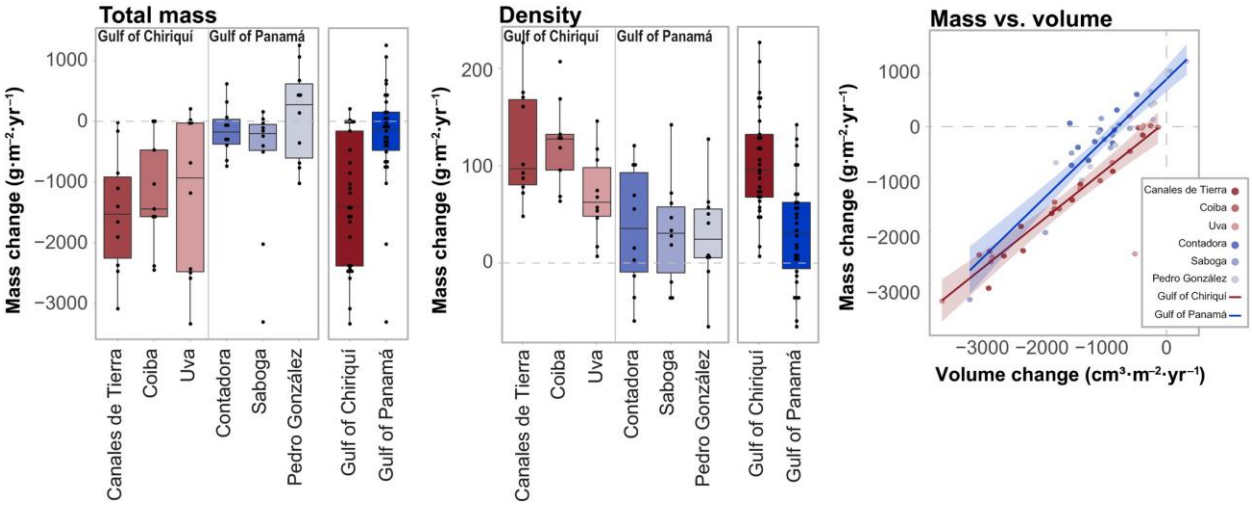

Figure 4. Changes in total mass and density of skeletal material that remained unbored by macroborers by site, and averaged across sites within each gulf. Total mass and density boxplots represent the medians (solid horizontal lines) and interquartile ranges (boxes). Error bars (whiskers) are 1.5 times the interquartile range. The plot on the right shows the relationships between change in mass and volume by site, with regressions conducted for each gulf (GoC, y = 0.944x + 48.3, r^2 = 0.82; GoP, y = 1.21x + 733, r^2 = 0.89). Values in all plots are time and surface-area standardized to represent rates of change per unit area.

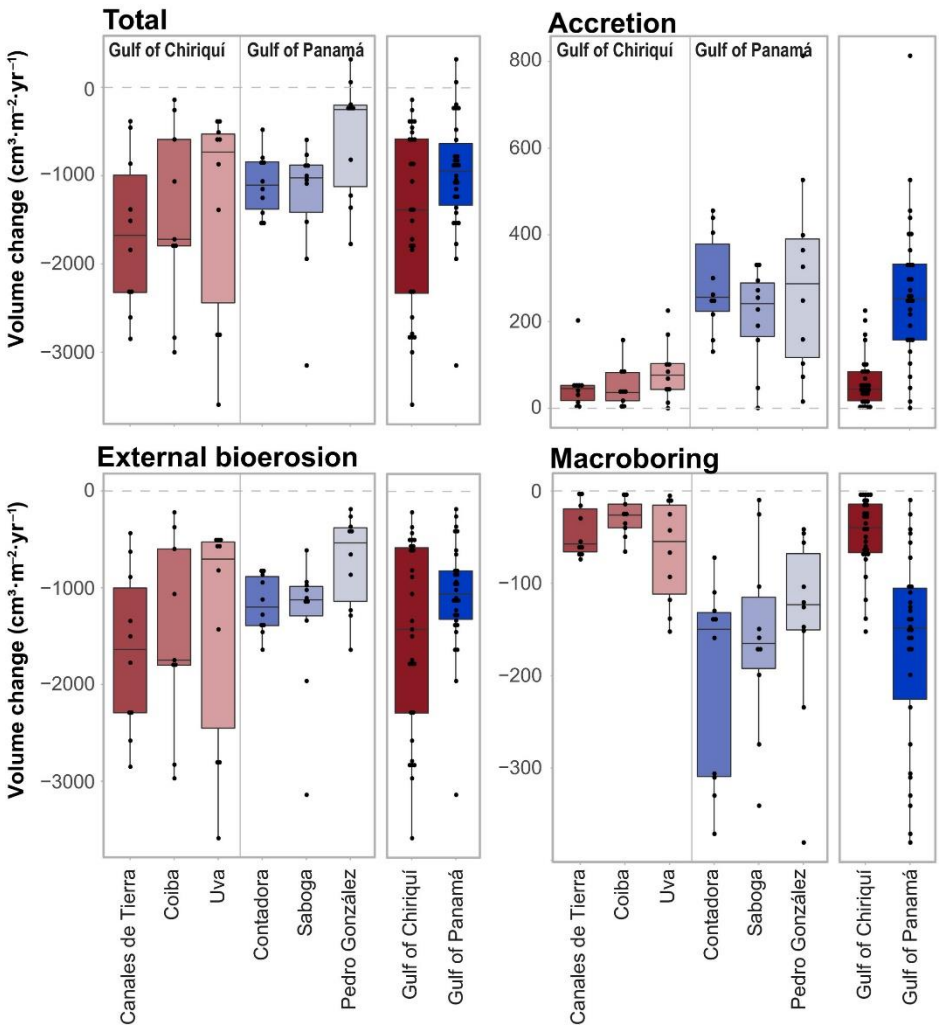

Figure 5. Total (net) volumetric change, accretion, macroboring, and external bioerosion of the bioerosion accretion replicates. Box plots represent the medians (solid horizontal lines) and interquartile ranges (boxes). Error bars (whiskers) are 1.5 times the interquartile range. Points represent significant outliers. Volumes that have been eroded are expressed as negative and newly accreted volumes are positive. No change in volume is marked as a horizontal dashed line. Data are summarized by both site and gulf, and are standardized by time and surface area to reflect rates of change in volume per unit area.

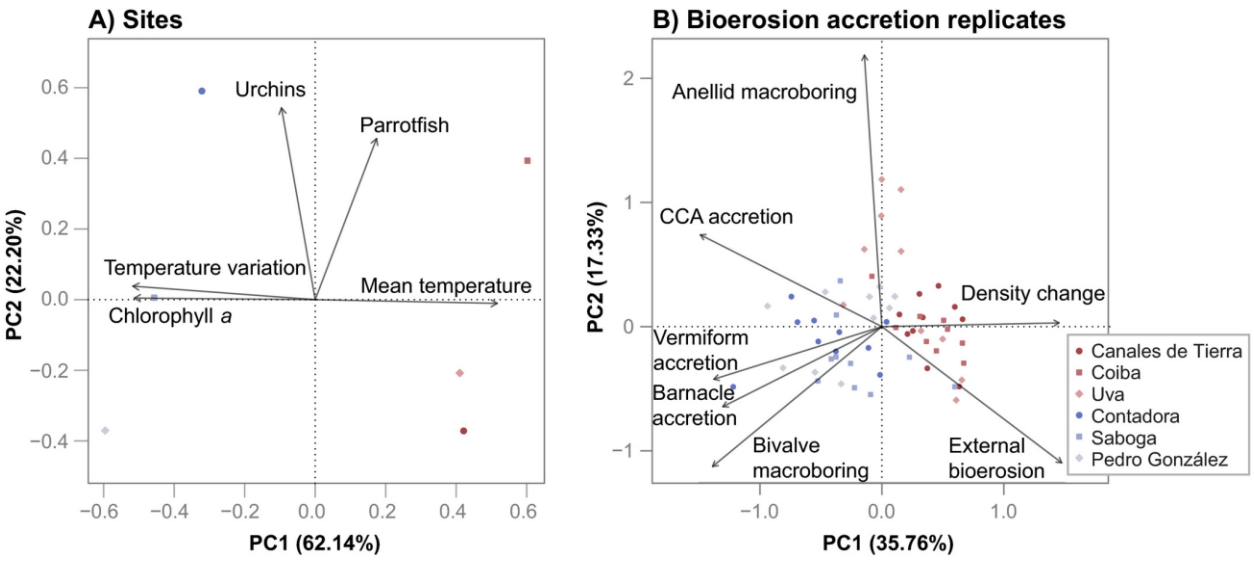

Figure. 6. Principal component analysis (PCA) of (A) sites and (B) carbonate blocks, based on environmental and accretion/erosion variables, respectively. In each PCA, sites/blocks are indicated by points, and variables by vectors. Point shapes/colors indicate site/gulf (red, Gulf of Chiriquí; blue, Gulf of Panamá). The coordinates of the vector arrowheads indicate the relative contributions of those variables to the first two PC axes, determined by the corresponding PC eigenvectors of each variables, which are scaled by 0.25 for clarity. (A) Gulfs differentiate on the first PC axis, which is primarily driven by mean temperature, temperature variation, and chlorophyll *a* concentration at each site. Sites further differentiate within gulfs according to grazer density. (B) Bioerosion accretion replicates largely differentiate by gulf on the first PC axis.

Appendix S1

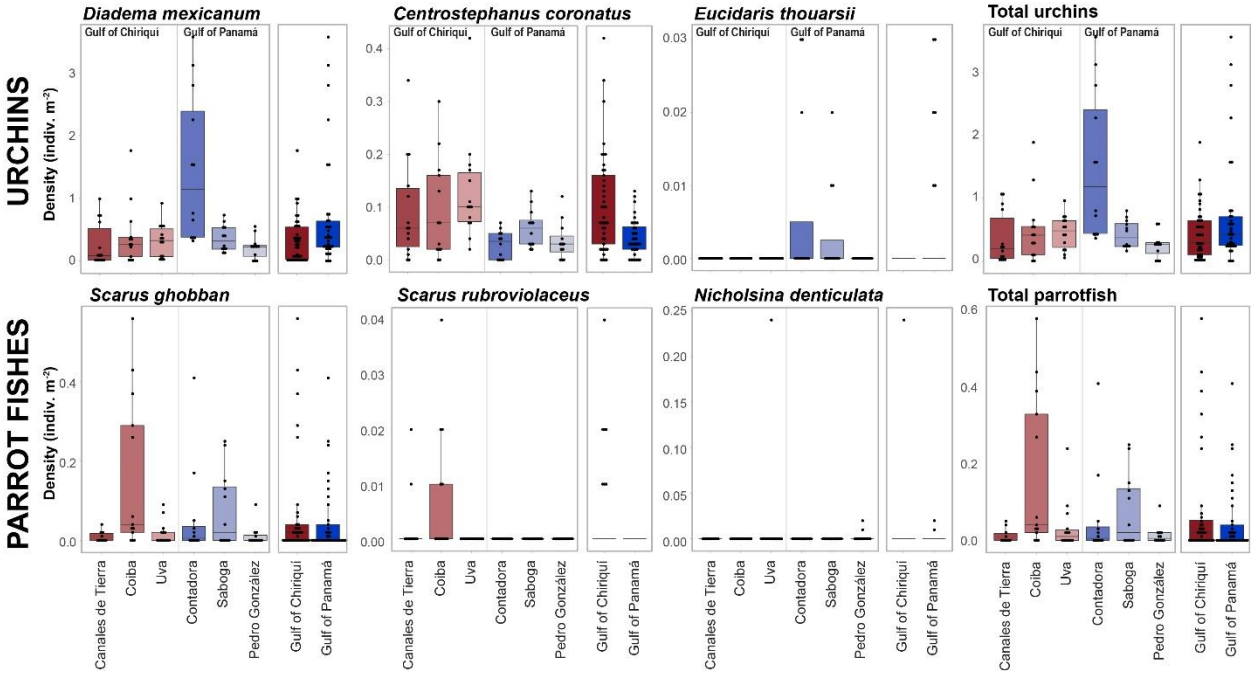

Figure S1. Densities of sea urchin and parrotfish species, as well as their total densities by site and gulf. Boxplots represent the medians (solid horizontals) and interquartile ranges (boxes). Error bars (whiskers) are 1.5 times the interquartile range. Some zero values are removed from the panels showing gulf averages, where exceptionally high numbers of points make it difficult to differentiate groups.

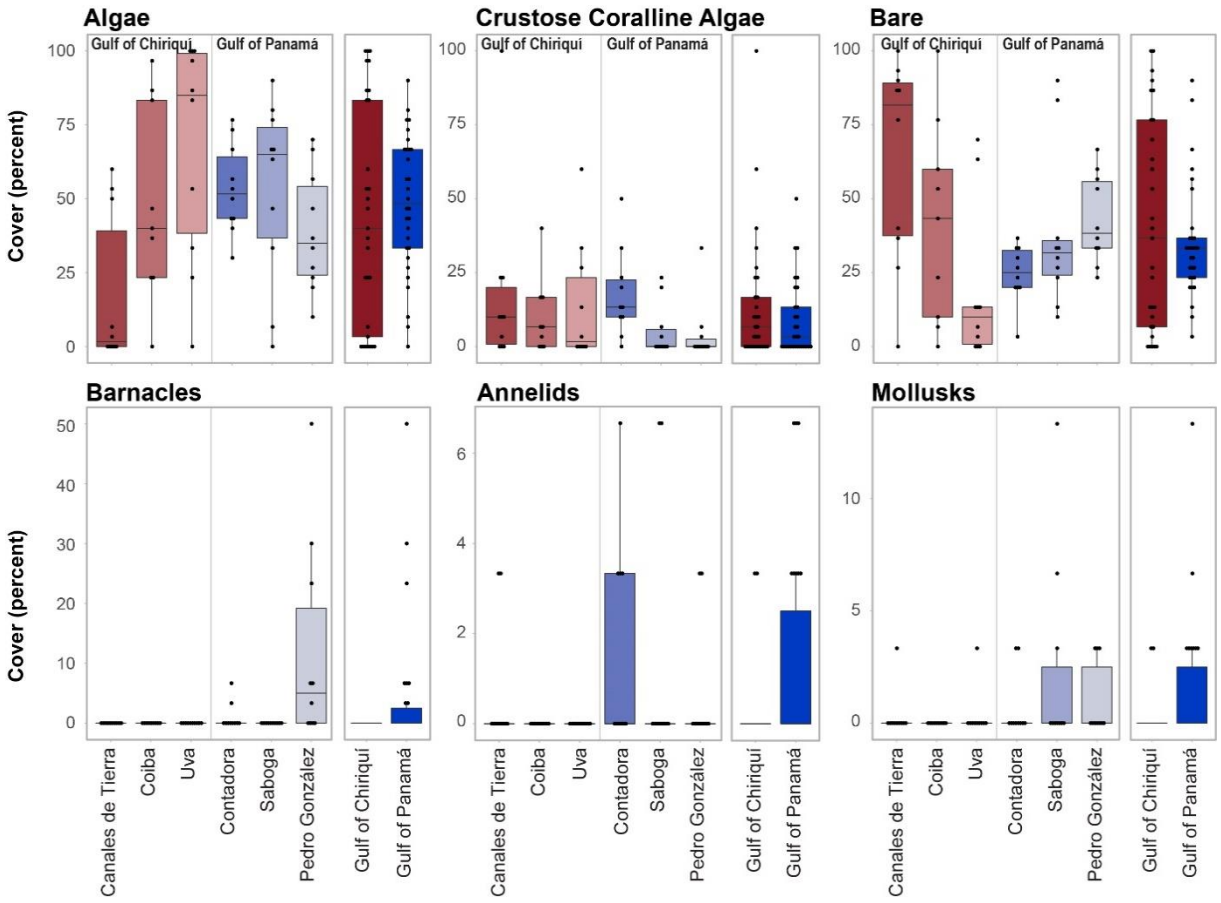

Figure S2. Community composition (percent cover) occupying the surface of bioerosion accretion replicates (BARs) at each site and within each gulf. Boxplots represent the medians (solid horizontals) and interquartile ranges (boxes). Error bars (whiskers) are 1.5 times the interquartile ranges. Some zero values are removed from the panels showing gulf averages, where exceptionally high numbers of points make it difficult to differentiate groups.

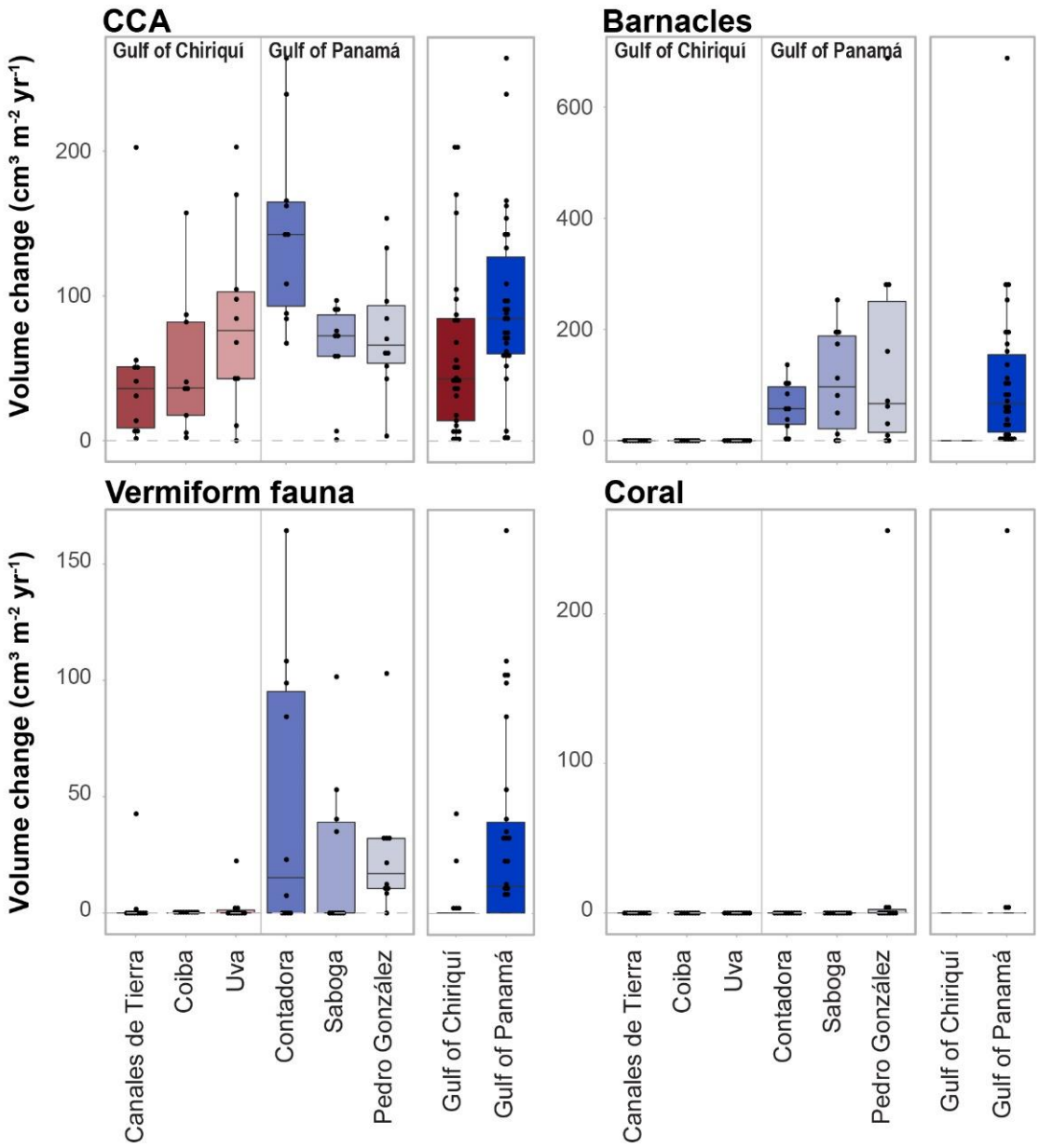

Figure S3. The total volume of carbonate accreted to the surface of bioerosion accretion replicates (BARs) by four groups of organisms. Boxplots represent the medians (solid horizontals) and interquartile ranges (boxes). Error bars (whiskers) are 1.5 times the interquartile ranges. Data are grouped by both site and gulf. Values are standardized by time and surface area to reflect rates of change in volume per unit area. CCA is crustose coralline algae. Some zero values are removed from the panels showing gulf averages, where exceptionally high numbers of points make it difficult to differentiate groups.

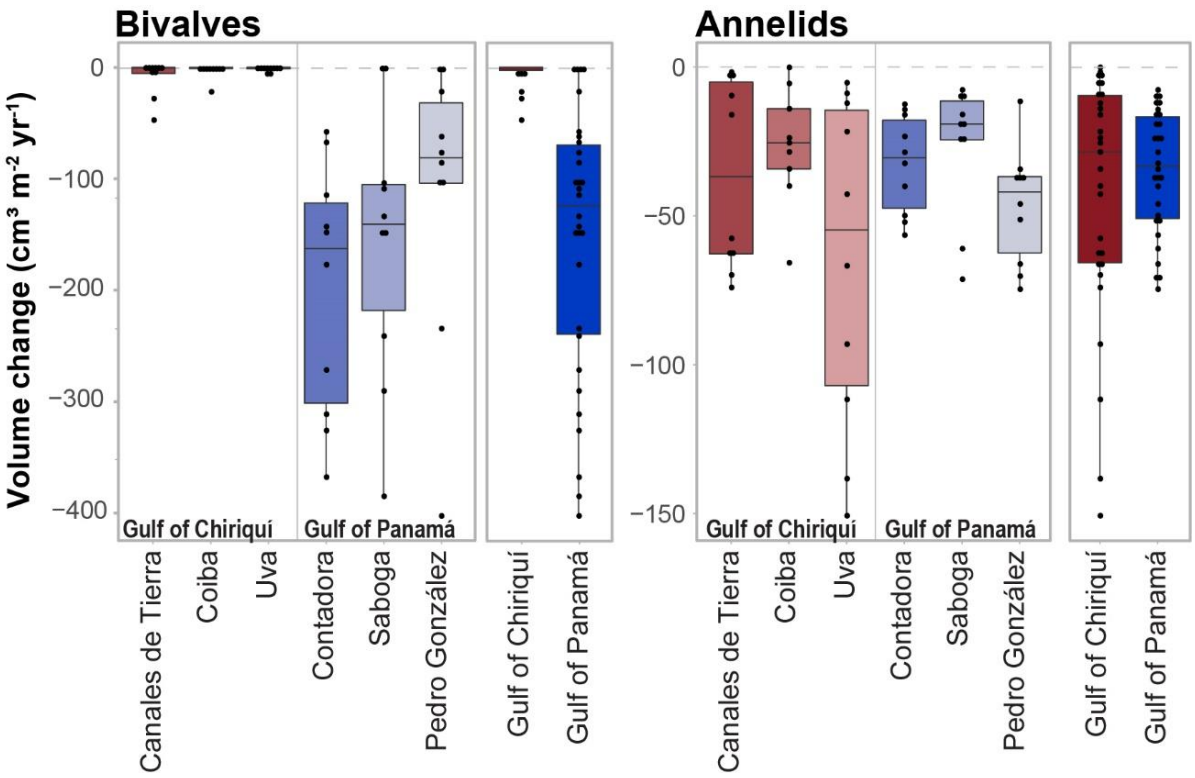

Figure S4. The total volume of carbonate eroded from within bioerosion accretion replicates (BARs) by two groups of macroboring organisms. Boxplots represent the medians (solid horizontals) and interquartile ranges (boxes). Error bars (whiskers) are 1.5 times the interquartile range. Data are averaged by both site and gulf, and are standardized by time and surface area to reflect rates of change in volume per unit area.

Table S1. Mean environmental conditions for each gulf and site by season, as well as the densities of grazing urchins and parrotfish. Standard deviations are in parentheses.

Site	Temperature (°C)	Min (°C)	Max (°C)	Chlorophyll-*a* (mg m^{-3})	pCO_2 (µatm)	Urchins (indiv. m^{-2})	Parrotfish (indiv. m^{-2})
Gulf of Chiriquí	28.8 (0.7)	25.6	31.0	0.51 (0.16)	527.4 (97.5)	0.43 (0.41)	0.08 (0.15)
Dry	28.9 (0.7)	25.6	30.8	0.48 (0.19)	487.6 (63.4)		
Wet	28.8 (0.7)	26.7	31.0	0.53 (0.14)	548.5 (105.5)		
Canales de Tierra	28.9 (0.7)	25.6	30.8	0.62 (0.27)		0.35 (0.42)	0.01 (0.02)
Dry	29.0 (0.8)	25.6	30.8	0.49 (0.10)			
Wet	28.9 (0.7)	26.7	30.8	1.06 (0.15)			
Coiba	28.9 (0.6)	26.2	31.0	0.58 (0.26)		0.50 (0.54)	0.17 (0.21)
Dry	28.9 (0.7)	26.2	30.5	0.61 (0.29)			
Wet	28.9 (0.6)	27.2	31.0	0.55 (0.24)			
Uva	28.6 (0.7)	25.9	30.5	0.50 (0.24)		0.45 (0.27)	0.04 (0.07)
Dry	28.8 (0.8)	25.9	30.3	0.42 (0.17)			
Wet	28.6 (0.7)	26.7	30.5	0.56 (0.28)			
Gulf of Panamá	27.4 (2.3)	17.9	29.8	1.32 (1.03)	572.8 (148.8)	0.73 (0.88)	0.05 (0.09)
Dry	25.1 (2.5)	17.9	28.7	1.69 (1.32)	649.3 (192.4)		
Wet	28.6 (0.6)	23.9	29.8	1.01 (0.61)	533.8 (100.4)		
Contadora	27.7 (2.0)	18.8	29.7	1.79 (1.33)		1.51 (1.17)	0.06 (0.12)
Dry	25.7 (2.3)	18.8	28.7	2.20 (1.53)			
Wet	28.7 (0.6)	23.9	29.7	1.21 (0.73)			
Saboga	27.3 (2.4)	17.9	29.5	2.24 (2.01)		0.42 (0.22)	0.08 (0.10)
Dry	24.9 (2.7)	17.9	28.5	2.86 (2.36)			
Wet	28.6 (0.6)	24.1	29.5	1.35 (0.92)			
Pedro González	27.2 (2.4)	18.5	29.8	2.51 (2.05)		0.25 (0.20)	0.01 (0.03)
Dry	24.7 (2.6)	18.5	28.3	3.25 (2.18)			
Wet	28.5 (0.7)	24.4	29.8	1.61 (1.55)			

Table S2. Mean community composition (percent cover) occupying the surface of bioerosion accretion replicates (BARs) at each site and averaged within each gulf. Standard deviations are in parentheses.

Site	Algae	CCA	Bare	Barnacles	Annelids	Mollusks
Gulf of Chiriquí	44.4 (37.9)	14.0 (22.0)	41.1 (36.2)	0.0 (0.0)	0.2 (0.9)	0.2 (0.9)
Canales de Tierra	17.3 (25.8)	18.0 (30.1)	63.7 (34.7)	0.0 (0.0)	0.7 (1.4)	0.3 (1.1)
Coiba	48.5 (33.2)	10.0 (13.0)	41.5 (34.3)	0.0 (0.0)	0.0 (0.0)	0.0 (0.0)
Uva	67.7 (37.3)	13.7 (20.4)	18.3 (26.1)	0.0 (0.0)	0.0 (0.0)	0.3 (1.1)
Gulf of Panamá	48.4 (23.2)	9.1 (12.9)	35.2 (19.7)	4.3 (11.0)	1.2 (2.2)	1.3 (2.9)
Contadora	53.3 (15.2)	17.7 (14.9)	24.7 (9.7)	1.0 (2.3)	1.7 (2.4)	0.7 (1.4)
Saboga	53.0 (30.8)	5.3 (8.9)	38.0 (27.1)	0.0 (0.0)	1.3 (2.8)	2.3 (4.5)
Pedro González	39.0 (20.4)	4.3 (10.4)	43.0 (15.0)	12.0 (17.0)	0.7 (1.4)	1.0 (1.6)

Table S3. Generalized Linear Model outputs for the main taxa present on the surface of the bioerosion accretion replicates (BARs). Sites are nested within gulfs. Distribution and Akaike Information Criterion (AIC) appear in parentheses next to each model.

	Estimate	Std. Error	t value	p
Algae (Gaussian, AIC = 568.45)				
(Intercept)	17.33	8.87	1.96	0.0558
Gulf of Panamá	21.67	12.54	1.73	0.0898
Coiba	31.19	12.88	2.42	0.0189
Uva	50.33	12.54	4.01	0.0002
Contadora	14.33	12.54	1.14	0.2581
Saboga	14.00	12.54	1.12	0.2692
CCA (Gamma, AIC = 412.59)				
(Intercept)	0.05	0.02	2.20	0.0320
Gulf of Panamá	0.13	0.09	1.53	0.1330
Coiba	0.04	0.05	0.77	0.4440
Uva	0.02	0.041	0.40	0.6925
Contadora	-0.13	0.09	-1.51	0.1361
Saboga	-0.03	0.11	-0.27	0.7912
Bare (Gamma, AIC = 552.00)				
(Intercept)	0.02	0.00	4.14	0.0001
Gulf of Panamá	0.01	0.01	1.09	0.2788
Coiba	0.01	0.01	1.14	0.2578
Uva	0.04	0.01	2.78	0.0075
Contadora	0.02	0.01	1.49	0.1420
Saboga	0.00	0.01	0.35	0.7261
Barnacles (Binomial, AIC = 35.47)				
(Intercept)	-2.06E+01	5.61E+03	0.00	0.9971
Gulf of Panamá	2.10E+01	5.61E+03	0.00	0.9970
Coiba	9.33E-09	8.15E+03	0.00	1.0000
Uva	9.33E-09	7.93E+03	0.00	1.0000
Contadora	-1.79	1.02	-1.76	0.0792
Saboga	-2.10E+01	5.61E+03	0.00	0.9970
Annelids (Binomial, AIC = 55.48)				
(Intercept)	-1.39	7.91E-01	-1.75	0.0795
Gulf of Panamá	-5.57E-17	1.12	0.00	1.0000
Coiba	-1.82E+01	3.58E+03	-0.01	0.9960
Uva	-1.82E+01	3.40E+03	-0.01	0.9957
Contadora	9.81E-01	1.02	0.96	0.3366
Saboga	-2.48E-16	1.12	0.00	1.0000
Mollusks (Binomial, AIC = 59.45)				
(Intercept)	-2.20	1.05	-2.08	0.0371
Gulf of Panamá	1.35	1.26	1.07	0.2840
Coiba	-1.64E+01	2.17E+03	-0.01	0.9940
Uva	-4.14E-16	1.49	0.00	1.0000
Contadora	-5.39E-01	1.05	-0.51	0.6075
Saboga	-9.21E-16	9.76E-01	0.00	1.0000

Table S4. Changes in the bioerosion accretion replicates (BARs), including general responses, as well as accretion and bioerosion of functional groups and taxa. Data are averaged by both site and gulf, and are standardized by time and surface area to reflect rates of change in volume per unit area. Mass and density are in g m^{-2} yr^{-1}, whereas all other values are based on volume and expressed as cm^3 m^{-2} yr^{-1}. Standard deviations are in parentheses.

	General responses			**Accretion**					**Bioerosion**			
	Mass	**Density**	**Total volume**	**Total**	**CCA**	**Barnacle**	**Verm.**	**Coral**	**External bioerosion**	**Total macro**	**Bivalve macro**	**Annelid macro**
Gulf of Chiriquí	-1328.2 (1074.0)	103.9 (54.2)	-1457.8 (1030.7)	62.8 (59.8)	60.2 (58.8)	0.0 (0.0)	2.5 (8.8)	0.0 (0.0)	-1473.3 (1003.5)	-47.3 (40.4)	-4.3 (10.5)	-43.0 (41.2)
Canales de Tierra	-1504.2 (998.5)	121.2 (57.8)	-1608.6 (872.6)	50.6 (57.2)	45.9 (58.8)	0.0 (0.0)	4.4 (13.4)	0.0 (0.0)	-1614.8 (831.0)	-44.4 (28.4)	-8.5 (16.1)	-35.9 (31.5)
Coiba	-1214.3 (917.2)	123.4 (45.5)	-1437.2 (1030.2)	51.7 (49.6)	51.5 (49.7)	0.0 (0.0)	0.1 (0.3)	0.0 (0.0)	-1459.6 (994.3)	-29.3 (20.8)	-3.0 (7.2)	-26.4 (19.6)
Uva	-1254.9 (1338.0)	69.2 (43.6)	-1325.5 (1247.0)	85.0 (69.6)	82.3 (65.2)	0.0 (0.0)	2.7 (7.0)	0.0 (0.0)	-1344.1 (1234.1)	-66.4 (56.0)	-1.3 (2.5)	-65.1 (55.4)
Gulf of Panamá	-232.4 (861.1)	31.8 (54.6)	-794.3 (669.1)	266.5 (166.5)	94.7 (60.6)	108.8 (138.8)	32.7 (43.5)	8.8 (46.6)	-871.0 (586.0)	-189.8 (118.7)	-154.7 (120.4)	-35.1 (20.6)
Contadora	-151.8 (416.9)	35.8 (62.6)	-858.3 (337.7)	286.2 (113.4)	146.4 (65.2)	61.0 (45.1)	48.6 (60.1)	0.0 (0.0)	-913.5 (323.1)	-231.0 (120.0)	-198.5 (112.1)	-32.5 (16.4)
Saboga	-659.5 (1116.7)	31.1 (54.6)	-1110.1 (822.1)	210.6 (113.6)	62.2 (33.6)	107.2 (92.6)	23.0 (34.5)	0.0 (0.0)	-1138.2 (800.5)	-182.4 (117.6)	-156.2 (120.8)	-26.2 (22.0)
Pedro González	114.1 (790.8)	28.5 (51.7)	-414.6 (614.1)	302.8 (241.2)	75.5 (43.9)	158.2 (215.1)	26.3 (29.2)	26.3 (80.6)	-561.4 (416.3)	-156.0 (118.2)	-109.3 (123.1)	-46.6 (19.4)

Table S5. Generalized Linear Model outputs for changes in the bioerosion accretion replicates (BARs) deployed at each site. Sites are nested within gulfs. Model outputs are grouped according to general responses, accretion and bioerosion. Distribution and Akaike Information Criterion (AIC) appear in parentheses next to each model.

	Estimate	Std. Error	t value	p
GENERAL RESPONSES				
Mass change (Gaussian, AIC = 987.05)				
(Intercept)	-1504.2	307.8	-4.9	9.90E-06
Gulf of Panamá	1618.38	435.4	3.7	0.0005
Coiba	289.9	447.3	0.6	0.5198
Uva	249.3	435.4	0.6	0.5693
Contadora	-265.9	435.4	-0.6	0.5440
Saboga	-773.6	435.4	-1.8	0.0813
Density change (Gaussian, AIC = 643.95)				
(Intercept)	121.2	16.8	7.2	2.08E-09
Gulf of Panamá	-92.7	23.8	-3.9	0.0003
Coiba	2.2	24.4	0.1	0.9280
Uva	-52.0	23.8	-2.2	0.0332
Contadora	7.3	23.8	0.3	0.7600
Saboga	2.6	23.8	0.1	0.9134
Total volume (Gaussian, AIC = 973.38)				
(Intercept)	-1608.6	274.2	-5.9	2.95E-07
Gulf of Panamá	1194.0	387.7	3.1	0.0033
Coiba	171.4	398.4	0.4	0.6687
Uva	283.1	387.7	0.7	0.4686
Contadora	-443.7	387.7	-1.1	0.2576
Saboga	-695.5	387.7	-1.8	0.0786
ACCRETION				
Total accretion (Gamma, AIC = -86.55)				
(Intercept)	15.8	4.0	4.0	0.0002
Gulf of Panamá	-13.1	4.0	-3.2	0.0020
Coiba	-0.3	5.7	-0.1	0.9546
Uva	-6.3	4.6	-1.4	0.1793
Contadora	0.2	1.0	0.2	0.8753
Saboga	1.2	1.2	1.0	0.3274
CCA accretion (Gamma, AIC = -22.40)				
(Intercept)	5.7	1.4	3.9	0.0002
Gulf of Panamá	-2.2	1.7	-1.3	0.1985
Coiba	-0.6	2.0	-0.3	0.7626
Uva	-2.5	1.6	-1.5	0.1391
Contadora	-1.7	1.0	-1.7	0.0983
Saboga	0.7	1.4	0.5	0.5987
Barnacle accretion (Gamma, AIC = -361.66)				
(Intercept)	6.9E+02	1.6E+02	4.4	5.87E-05
Gulf of Panamá	-6.9E+02	1.6E+02	-4.3	6.44E-05
Coiba	-8.9E-12	2.3E+02	0.0	1
Uva	-9.1E-12	2.2E+02	0.0	1

Table S5. Generalized Linear Model outputs for changes in the bioerosion accretion replicates (BARs) deployed at each site. Sites are nested within gulfs. Model outputs are grouped according to general responses, accretion and bioerosion. Distribution and Akaike Information Criterion (AIC) appear in parentheses next to each model.

Contadora	6.8	2.7	2.5	0.0162
Saboga	2.0	1.8	1.2	0.2520
Vermiform fauna accretion (Gamma, AIC = -208.78)				
(Intercept)	30.4	15.1	2.0	0.0488
Gulf of Panamá	-24.4	15.4	-1.6	0.1189
Coiba	121.3	80.8	1.5	0.1388
Uva	14.6	27.0	0.5	0.5902
Contadora	-2.7	3.4	-0.8	0.4310
Saboga	0.8	4.5	0.2	0.8537
BIOEROSION				
External bioerosion (Gaussian, AIC = 967.56)				
(Intercept)	-1614.8	261.0	-6.2	9.09E-08
Gulf of Panamá	1053.3	369.1	2.9	0.0062
Coiba	155.2	379.2	0.4	0.6840
Uva	270.6	369.1	0.7	0.4666
Contadora	-352.1	369.1	-1.0	0.3445
Saboga	-576.8	369.1	-1.6	0.1240
Total macroboring (Gaussian, AIC = 704.62)				
(Intercept)	-44.5	28.1	-1.6	0.1198
Gulf of Panamá	-111.5	39.8	-2.8	0.0070
Coiba	15.1	40.8	0.4	0.7128
Uva	-22.0	39.8	-0.6	0.5831
Contadora	-75.0	39.8	-1.9	0.0646
Saboga	-26.5	39.8	-0.7	0.5082
Bivalve macroboring (Gaussian, AIC = 699.44)				
(Intercept)	-8.5	26.9	-0.3	0.7527
Gulf of Panamá	-100.8	38.0	-2.7	0.0106
Coiba	5.5	39.1	0.1	0.8878
Uva	7.2	38.0	0.2	0.8500
Contadora	-89.1	38.0	-2.3	0.0230
Saboga	-46.9	38.0	-1.2	0.2234
Annelid macroboring (Gamma, AIC = -38.78)				
(Intercept)	4.1	0.9	4.5	4.33E-05
Gulf of Panamá	-0.9	1.2	-0.8	0.4317
Coiba	1.4	1.6	0.9	0.3721
Uva	-1.8	1.1	-1.7	0.0910
Contadora	1.3	1.2	1.1	0.2854
Saboga	2.4	1.4	1.7	0.1023